

Progress in Shock Wave/Boundary Layer Interactions

D.V. Gaitonde*

*Mech. and Aerosp. Eng. Dept.
The Ohio State University
Columbus, OH*

Abstract

Recent advances in shock wave boundary layer interaction research are reviewed in four areas: i) understanding low frequency unsteadiness, ii) heat transfer prediction capability, iii) phenomena in complex (multi-shock boundary layer) interactions and iv) flow control techniques. Substantial success has been achieved in describing the phenomenology of low frequency unsteadiness, including correlations and coherent structures in the separation bubble, through complementary experimental and numerical studies on nominally 2-D interactions. These observations have been parlayed to propose underlying mechanisms based on oscillation, amplification and upstream boundary layer effects. For heat transfer prediction capability, systematic studies conducted under the auspices of AFOSR and RTO-AVT activities have shown that for axisymmetric laminar situations, heat transfer rates can be measured and in some cases be predicted reasonably accurately even in the presence of high-temperature effects. Efforts have quantified uncertainty of Reynolds averaged turbulence models, and hybrid methods have been developed to at least partially address deficiencies. Progress in complex interactions encompass two of the major phenomena affected by *SBLI* in scramjet flowpaths: unstart and mode transition from ramjet (dual mode) to scramjet. Control studies have attempted to leverage the better understanding of the fundamental phenomena with passive and active techniques, the latter exploiting the superior properties of newer actuators. Of interest are not only reduction in separation and surface loads, but also the spectral content. Finally, *SBLI* studies have benefited handsomely from successful ground and flight test campaigns associated with the *HIFIRE-1* and *HIFIRE-2* campaigns, results from which are woven into the discussion, as are limitations in current capability and understanding.

I. Introduction

Shock-wave boundary layer interactions (*SBLI*) occur in all practical transonic, supersonic and hypersonic vehicles. In one of the earliest reviews on the subject, Green¹ identifies four important situations: transonic aerofoils, high-speed inlets, nozzles at off-design conditions, and near control flaps. This paper examines the last three, where typically the boundary layer, which could be laminar, transitional or turbulent (*STBLI*), on a surface encounters a shock wave, generated perhaps by an adjacent or opposite surface. The practical impact can be very harmful and must be factored into design tradeoffs. On the exterior of the aircraft, *SBLI* can cause loss of control authority, peaks in surface thermomechanical loading, and unsteadiness of a nature that can induce adverse structural response. In internal flows, they can enhance pressure losses and distortion, and in extreme cases could trigger potentially catastrophic events leading to unstart. From a fundamental fluid dynamics perspective, these viscous-inviscid interactions generate a diverse range of phenomena. In strong interactions, the flow separates to yield vortical structures, turbulence amplification and modifications to the structure parameter. Multiple unsteady phenomena simultaneously impose their signature on the spectrum.

The importance of *SBLI* is reflected in the emphasis they have received. They are an important component of the National Hypersonics Foundational Research Plan, developed by AFOSR, NASA and Sandia, which provides a framework of the main areas in hypersonics research. The Research and Technology Office, Air Vehicle Technology (RTO/AVT) has been an integral part of that development (see Ref. 2). Efforts from European, Australian and Japanese

*John Glenn Professor, Fellow AIAA, gaitonde.3@osu.edu

programs have focused on varied aspects of *SBLI* and have greatly contributed to fundamental and applied advances over the last decade.

Numerous review articles provide chronological snapshots of the state-of-the art at different times over the past several decades with extended discussions of the physics as well as experimental and numerical techniques.^{3–9} Among the latest is by Dolling,¹⁰ which focuses especially on elaborating on outstanding issues and suggests next steps in the development and application of simulation tools and measurements. Other recent compendiums of *SBLI* research may be found in Refs. 11, 12.

The fundamental physics of *SBLI* are best examined in canonical situations. Some of the more common configurations are shown in Fig. 1. Extensive measurements are available for these, including time mean and unsteady measurements of surface pressure, skin friction coefficient, heat transfer rate, particle image velocimetry (*PIV*) and field Pitot pressure surveys. Qualitative measurements include schlieren images of shock structure and surface oil flow visualizations. A few representative articles may be found in Refs. 13–18. The nominally 2-D configurations comprised of impinging shocks (Fig. 1(a)) and compression ramps (angle θ , Fig. 1(b)) represent perhaps the most studied problems, although in practice three-dimensional effects associated with sidewalls and corner flows often contaminate such observations. The axisymmetric counterpart is the cylinder flare or a double cone (Fig. 1(c)). Sweep (angle λ) can be introduced into the compression ramp to yield the swept ramp (or corner), Fig. 1(d). Further, increasing θ to 90° yields the (single) sharp-fin (Fig. 1(e)) while positioning an opposing fin generates the double-fin configuration (Fig. 1(f)). A blunt fin (not shown) on plate has also been extensively explored as a surrogate for protuberances. Three-dimensionality can be introduced into axisymmetric situations with angle of attack or for example as in Ref. 17 by off-setting the axis of one component relative to the other. The internal flow situation (Fig. 1(g)) is representative of dual-mode or scramjet flowpaths.

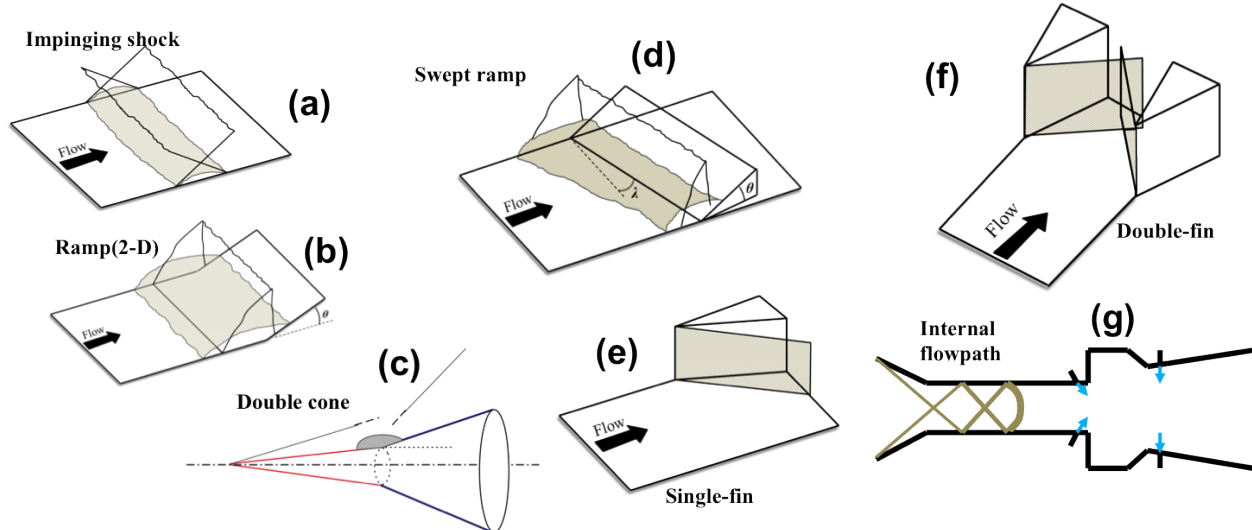


Figure 1. Canonical configurations employed for fundamental studies of *SBLI*

An especially exciting development has been the success of the HIFiRE ground and flight test campaigns, with associated simulations. The first two flight test articles, denoted *HIFiRE-1* and *HIFiRE-2* are shown in Fig. 2. Each has significant *SBLI* effects. The coupling of these tests to advanced computations and postprocessing has greatly fulfilled their discovery objective: key results pertinent to *SBLI* are woven in the main discussion thrusts below. *HIFiRE-1*, shown in Fig. 2(a), was successfully flown in March 2010 on a sounding rocket stack. Details of the program, including the evolution and establishment of the main parameters and flight trajectory, pre-flight ground test data acquisition at CUBRC and NASA Langley, diagnostics placement, and assessment of the actual flight data has been provided in articles by Dolvin, Kimmel, Adamczak *et al.*^{19–21} The *HIFiRE-2* test article, shown in Fig. 2(b) is designed to isolate key aspects of dual-mode scramjet operation through mode transition. Its successful launch was conducted in May 2012. Further details may be found in Refs. 22–25.

To motivate the discussion, Section II starts by highlighting the key aspects of the mean flow obtained in some of the canonical forms of Fig. 1. The main issues of interest are then binned in a manner that follows the overall framework of Ref. 10. Even a cursory exploration of the recent literature suggests that significant progress in measurement and computation have indeed led to much better understanding of the fundamental physics of *SBLI*. In particular, Large Eddy Simulations (LES) and Direct Numerical Simulations (DNS) have become commonplace, as have ever

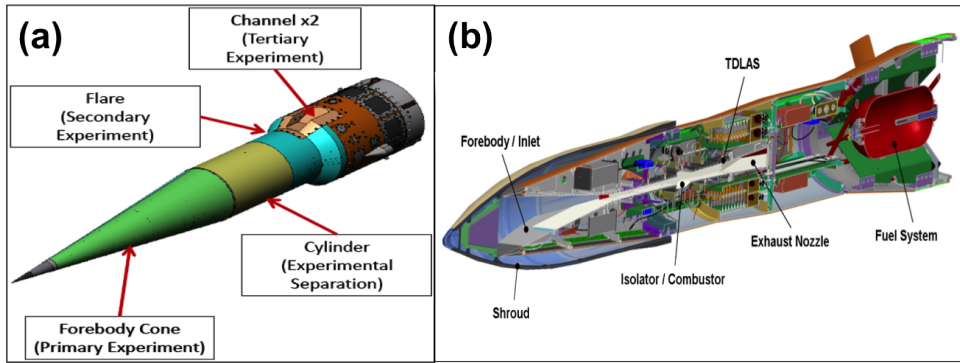


Figure 2. Flight test articles: (a)HIFiRE-1; (b)HIFiRE-2

more accurate unsteady measurements of the flow field without and with high temperature effects.

It is necessary to limit the scope of the paper to maintain a degree of conciseness. Although recent advances in diagnostic and computational tools have played a crucial role in recent research, these are not the focus of the paper. Rather, the primary emphasis of this paper is on the physics of *SBLI*, though some importance is given to accuracy of numerical methods in the context of heat transfer rate prediction, since this is a major thrust of some current research programs. The figures employed to illustrate salient points are taken from the work of the author and his collaborators mainly because of their ready availability. Transitional interactions are not discussed although such *SBLI* interactions have been examined experimentally (for example near a blunt fin in a supersonic stream by Murphree *et al*²⁶) and computationally (for example an impinging shock case by Teramoto²⁷). Finally, in the interest of brevity, many insightful efforts could not be included and some conclusions are stated without elaboration of some of the qualifications noted in the cited work: there is thus a necessary if undesirable degree of generalization.

The four main areas in which recent advances are reviewed are as follows:

- a. Unsteadiness: Perhaps the most significant breakthroughs in understanding the phenomenology and physics of *SBLI* since the publication of Ref. 10, have been in the area of unsteadiness. Numerous studies have explored the genesis of the prominent low frequency component inherent in *SBLI*, *i.e.*, frequencies at levels well below the scales associated with turbulence in the boundary layer. This low frequency component is accompanied by separation shock foot movement and spanwise shock rippling, and has been documented to varying extent for all canonical configurations of Fig.1.²⁸⁻³² A series of closely coordinated computational and experimental studies during the last decade, focused on nominally 2-D configurations, has provided plausible explanations for the observations. Results from these efforts, are summarized in Section III. The structural differences between 2-D and 3-D separation, specifically closed bubbles in the mean flow in the former versus open structures with little or no reversed flow in the latter as discussed in Section II, are then employed to comment on factors in extending the analysis to 3-D flows.
- b. Heat transfer rates: The second major well known difficulty has been the determination of heat transfer rates (and skin friction coefficients) and the dynamics that establish the observed values. The classical preferred approach, suitable for engineering purposes, has been to perform parametric studies whose results were then assimilated into empirical correlations. During the last decade or so however, carefully conducted *CFD*-friendly experiments have been performed with highly reliable and accurate diagnostics in simple configurations with complex flowfields, such as the hollow cylinder and double cone. Tightly coordinated and well organized computational exercises, some blind in nature, have shown that the heat transfer rates under laminar conditions, even with high temperature effects, can often be computed accurately enough with adequate mesh support and if the freestream conditions are properly characterized. These results are summarized in Section IV, followed by a discussion of issues related to determination of *turbulent* heat transfer rates, about which much remains to be learned. Progress has been made however in quantifying uncertainty of Reynolds averaged methods, and in the development of hybrid approaches. The 3-D flow structure discussed in Section II is again employed to highlight pertinent dynamics likely to be of importance going forward.
- c. Complex configurations: The increasing pace of research on scramjet development is exemplified by the active HIFiRE-2 and X-51 programs. Extensive ground test results are available from the former. Some of the main activities in this area, including experiments in the dynamics of unstart, and simulations in mode transition are presented in Section V.

d. Control: The traditional approach for *SBLI* control has been through bleed techniques, which alter the near wall low energy region to mute the deleterious effects of the interaction. The search for a more optimal solution has taken several directions, including passive (*e.g.*, microramps with and without auxiliary bleed) and active (*e.g.*, plasma-based or microjet) control techniques. The combination of a better understanding of the unsteadiness and the development of new high-bandwidth actuators has led to strategies that seek to leverage fluid instabilities with small disturbances of suitable spectral characteristics with more potential for scalability. Some key results are summarized in Section VI.

II. Two dimensional versus three-dimensional flow structure

As a framework for further discussion, here we highlight some key features of mean 2-D and 3-D flows in select canonical *SBLIs*.

Nominally 2-D flows: Figure 3(a) shows a schematic of the overall expected *mean* flow features of a separated impinging shock configuration. Inside the boundary layer, the shock typically bends as it encounters lower Mach

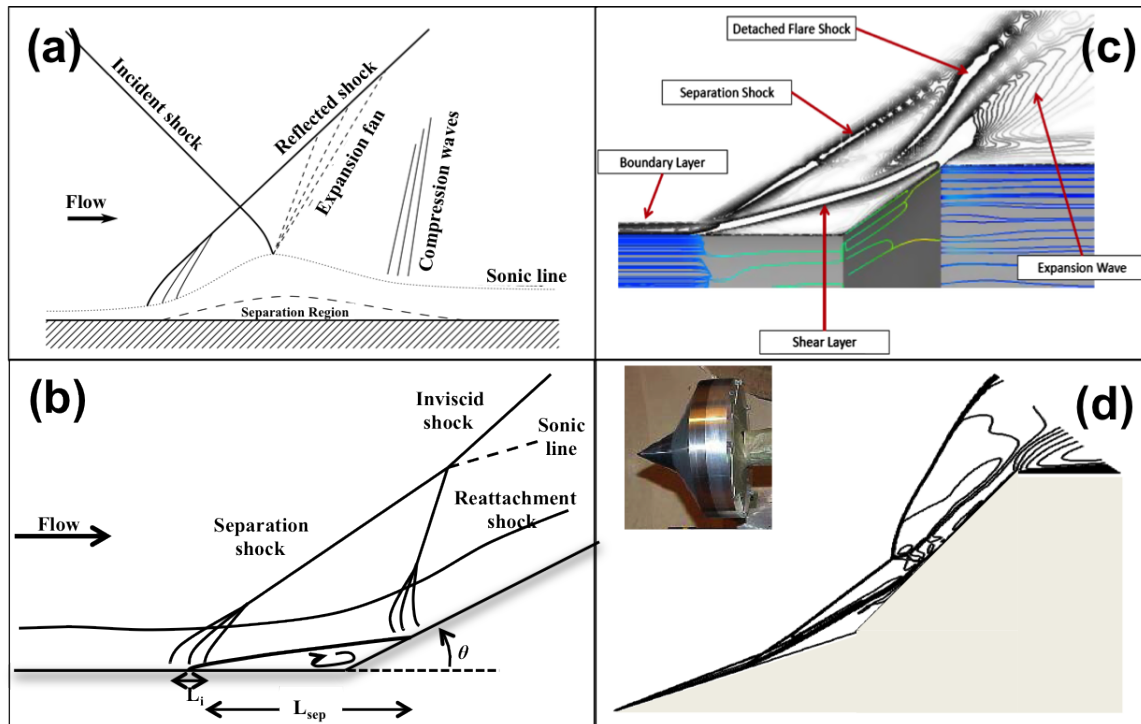


Figure 3. Aspects of flow structure in 2-D and axisymmetric interactions (a) impinging shock (2-D); (b) compression corner (2-D); (c) cylinder-flare (axisymmetric); (d) double-cone (axisymmetric)

numbers and ultimately breaks up into a compression fan³³ and a reflected shock develops as shown. For a given boundary layer, if the shock is strong enough, separation occurs. The compression corner flow shown in Fig. 3(b) has a single major shock associated with the ramp. However, the dynamics in terms of unsteadiness and separation is generally similar to the impinging shock (see Ref. 4 for a discussion on the differences between the two types of interactions). The length of the separation region, L_{sep} , and the incoming boundary layer thickness are the two larger length scales in the flow.

SBLI in canonical axisymmetric situations are shown in Figs. 3(c) and (d). The former is taken from Ref. 34 on the *HIFiRE-1* configuration discussed in more detail below. The flow represents the counterpart of the 2-D compression ramp, with similar topological features, except for the addition of a shoulder which is necessary in practical situations. Frame (d), taken from Ref. 35 is the *laminar* Mach 9 flow past the double-cone $25^{\circ} - 55^{\circ}$ configuration measured by Holden *et al.*^{36,37} The flow structure for this particular case has been couched in Ref. 35 in terms of a type V interaction of Edney.³⁸ Briefly, the two cones yield individual shocks linked at two triple points with a connector shock. A shear layer emanates from the aft triple point, effectively separating the subsonic flow from the near-wall supersonic jet. The viscous interaction associated with the reattachment shock is similar to that described for transonic interactions.³⁹ Comments on turbulence in such flows are deferred to Section IV.

3-D swept interactions: Even in nominally 2-D flows such as those just discussed, three-dimensionality is often an

issue of interest because of the finite wind tunnel size. Experimental constraints frequently yield unintended three-dimensional effects associated with sidewalls and corner flows.^{40,41} In an impinging shock flow for example, the generator used to initiate the incident shock necessarily results in a swept shock interaction with the sidewall boundary layer, and indeed, many of the basic features obtained as parasitic effects in 2-D interactions can be explained as 3-D interaction features, which are now discussed.

Although there is much unknown about unsteadiness and heat transfer rates in 3-D interactions, a clear understanding of the *mean* 3-D flowfield has been obtained from experiments and Reynolds Averaged Navier-Stokes (RANS) approaches, based on *carefully tailored* eddy viscosity models over a wide range of Mach and Reynolds numbers (see e.g., Refs. 42–45). Some of the main evidence for this assertion is shown in Fig. 4 for the double fin configuration.^{46,47} Frame (a) shows surface oil flow patterns, which represent the footprint of the 3-D flow field for a Mach 4 flow. The

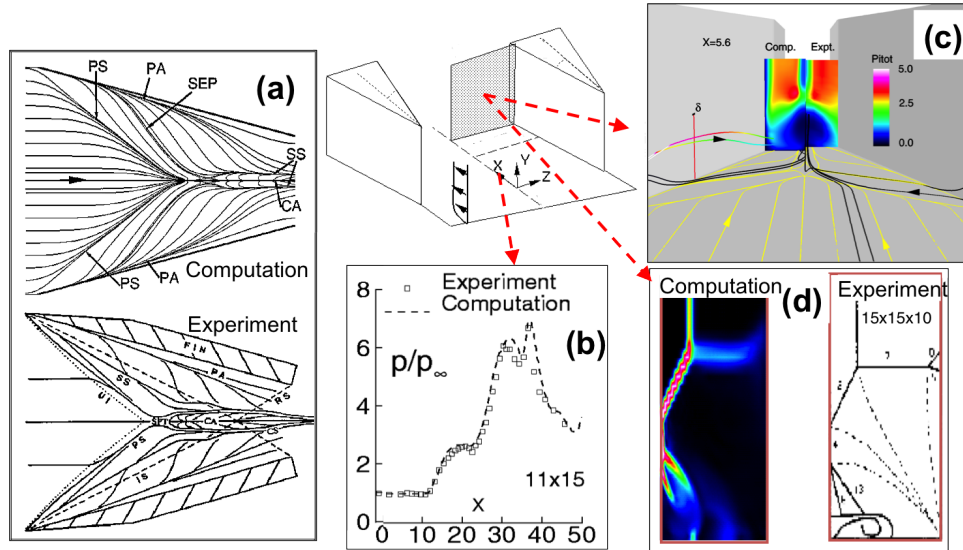


Figure 4. Comparison of computation and experiment for 3-D double-fin interactions. Experimental data taken from Refs. 44, 48, 49. (a) Surface oil flow; (b) surface pressure; (c) Pitot pressure on crossflow plane; (d) shock structure

principal lines of coalescence (separation) and divergence (attachment) are similar in computation and experiment. Frame (b) shows surface pressure comparison along the centerline of an asymmetric interaction induced by fins at 11° and 15° angles of attack. Frame (c) shows Pitot pressure on a cross-flow plane in Mach 8 flow, with some superposed streamlines on the surface as well as in the field. The main feature is a low energy region in the center of the channel. Frame (d) shows the computed and experimentally deduced shock structure in a triple fin interaction, where in addition to 15° fins, the plate is deflected at 10°. Each experimental shock feature is readily evident in the simulations. At even higher strengths, additional lines of separation and attachment appear in the flow. For example, as shown in Ref. 50, secondary separation and attachment are observed between the primary separation and attachment lines. Furthermore, in such strong SBLI, an irregular shock reflection appears in the inviscid region (see Ref. 51).

The remarkable accuracy with which the mean flow structure is reproduced by simulations is associated with the fact that after separation, the flow away from the walls is essentially inviscid rotational⁵² and thus, the flow is independent of eddy viscosity in much of the domain away from the walls. Indeed as discussed further below, downstream of separation, the vorticity distribution (again, only in regions away from the wall) is mostly dependent on its distribution in the incoming boundary layer: RANS approaches are designed to match these values and the overall flow structure can be captured quite accurately with a good numerical algorithm. We reiterate that heat transfer rates and unsteadiness are not captured by RANS methods,⁸ and remain outstanding issues to date for 3-D interactions.

Figure 5(a) shows the structure of a Mach 4 flow past a double-fin, together with corresponding surface streamlines in frame (b). Four regimes have been identified. The upstream boundary layer separates from the plate at the primary line of separation and does not reattach. Rather it becomes narrow and archlike, forming the bounds of the low energy region of Fig. 4(c). This facilitates attachment of fluid from the sides near the fin-plate juncture (at the primary line of attachment), which then sweeps span-wise and separates from the downstream side of separated boundary. For the single fin and swept compression corner interactions, the only other item of interest is the corner vortex whose footprint lies between the primary line of attachment and the corner. This vortex can impact measurements of nominally 2-D interactions as further discussed below. For the double fin, the region over the plate near the centerline is occupied by two relatively small longitudinal vortices.

This description highlights the profound distinction between 2-D and 3-D separated flows and the manner in

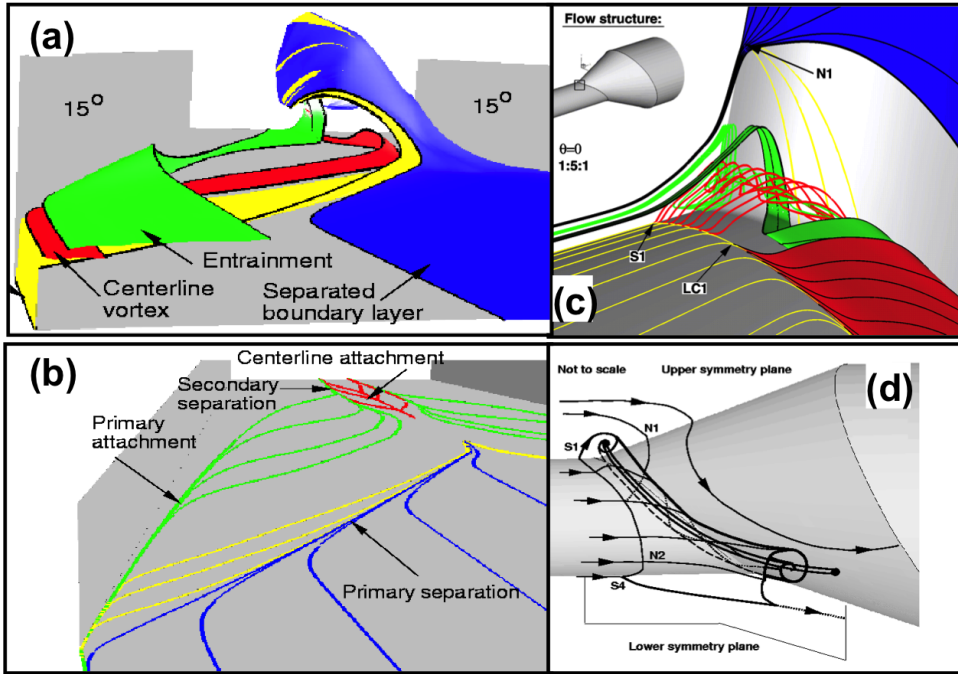


Figure 5. Three dimensional flow fields: (a) double-fin flow; (b) surface streamline pattern for double-fin flow; (c) flowfield near upper symmetry plane in cylinder-offset flare interaction; (d) schematic of vortical structure in cylinder-offset flare interaction

which it impacts the extension of results from the former to the latter. A major difference is that there is no bubble (or recirculating fluid region) in the 3-D case even in the time-mean sense. Indeed, for the single fin, there is no reversed flow at all, while for the double fin, it is restricted to a very small region near the centerline.

The flow past 3-D circular cross-section geometries also displays an open structure. Figure 5(c) and (d) shows a cylinder-flare configuration in which the flare axis is displaced relative to that of the cylinder. The experiments and simulations are discussed in Refs. 17 and 53 respectively. Again, the surface oil flow, pressure and overall flow structure (but not C_f) are accurately reproduced by RANS methods and careful analysis of the computed flow reveals a vortical structure whose legs wrap around the cylinder-flare juncture before being vented downstream as shown in Fig. 5(d).

III. Unsteadiness

As noted earlier, in this context, the term unsteadiness refers to frequencies of relatively high amplitudes in bands which are an order of magnitude or more lower than those associated with fine-scale turbulence in the incoming boundary layer. The problem of unsteadiness, in both nominally 2-D and 3-D circumstances has been the focus of experimental studies at speeds ranging from transonic to hypersonic over the course of several decades – see e.g., Refs. 1,54 for early descriptions – and key results from those and subsequent efforts are summarized in the reviews of Refs. 7, 10.

Since the publication of Ref. 10, sustained synergistic computational and experimental efforts have been conducted on the study of nominally 2-D situations, including both the ramp and impinging shock flows. Collectively, these have discounted the possibility that this was some unknown wind tunnel manifestation and indeed, the phenomenon has also been obtained in the *HIFIRE-1* flight test as discussed below. A particularly noteworthy coherent effort was performed under the UFAST (Unsteady eFfects of shock wAve induced Separation) project, which had this problem as one of its three major focus areas. Reference 12 describes many of the experimental and computational results from the study. The parameters range from Mach numbers of 1.7, 2.0 and 2.5 based on measurements at *TU Delft*, *ITAM* and *IUSTI* respectively, at a wide range of Reynolds numbers.

The overall implication of this recent work is that the phenomenology of unsteadiness has been clarified and mechanisms that explain the observations have been proposed, though there remain some nuances in the details, perhaps as a matter of semantics: the task is particularly difficult because the dynamics of the highly subsonic separated flow region makes causation and correlation difficult to separate, with a similar consideration for mechanisms that initiate or sustain the unsteadiness. We summarize first the observations and then the main proposed mechanisms.

The lower frequency motions are manifested in several macroscopic ways. Some of these features are illustrated

in Fig. 6 taken from Ref. 55 where a Mach 2.3 flow is considered with an impinging shock generated by a 9° wedge to reproduce the experiments of Refs. 56,57. Frame (a) shows the boundary layer with an artificial schlieren together with impinging and reflected shocks as isolines. Experimental and unsteady simulation data from various cited sources show large scale movement of the separation shock, and three-dimensionality is observable as rippling of the separation shock front in the spanwise direction. These effects are detected in appropriately placed pressure transducers on the plate surface. Near the foot of the separation (or reflected) shock, such measurements show an essentially bimodal distribution depending on whether the shock is upstream or downstream of the transducer. There is an accompanying change in the size of the separation region, with disturbances radiating along the reflected shock as well. The variation

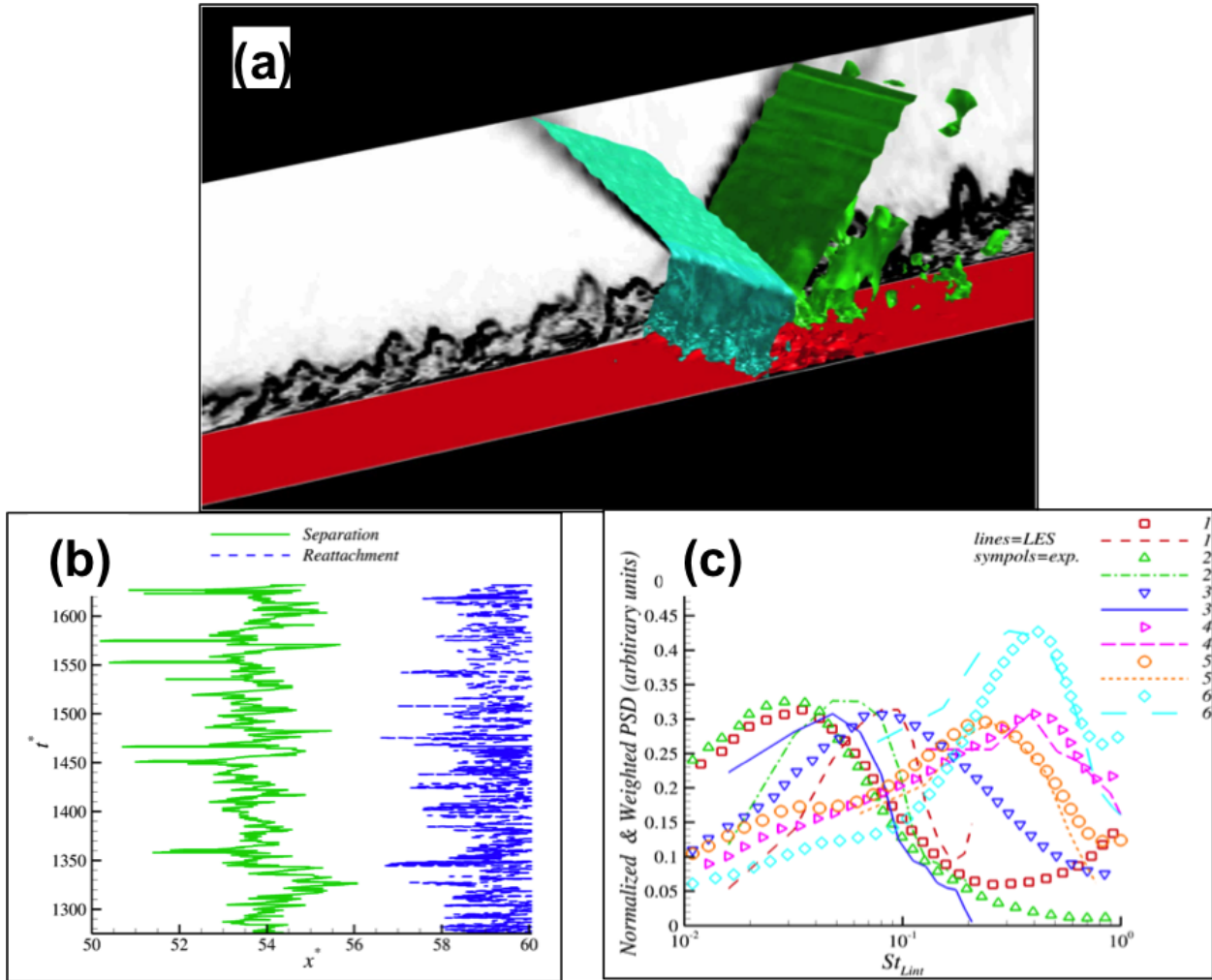


Figure 6. Elements of unsteadiness in impinging shock SBLI⁵⁵ (a) Schlieren of boundary layer and isolines to show shock structure; (b) separation and attachment location at different instants on centerplane of simulation; (c) low frequency signal at different points in the interaction

of the separation point with time at the central location of the domain, Fig. 6b, shows a large, almost 6δ streamwise range. The normalized and weighted power spectral density of the pressure signal on the surface is shown in Fig. 6(c) at several locations: station 1 is 3δ upstream of the mean separation point, while station 6 is about 2δ downstream of attachment. There is clearly a broad band character, with an increasing peak frequency as one proceeds downstream. Simulation values are first low pass filtered and then processed using Welch's method with a Hamming window. These predict the correct trends and are very accurate at the higher frequencies inside the interaction, but show greater error at the lower frequencies because of fewer cycles in the sampled record.

Some of the major efforts that have informed the current understanding are now discussed, considering first experiments and then simulations. Ganapathisubramani *et al*⁵⁸ measured several quantities in the upstream boundary layer at Mach 2, to show the existence of long streamwise structures in the boundary layer exceeding 8 boundary layer lengths. These correlated quite well with the main observed features of the unsteadiness. Dupont *et al*⁵⁹ used PIV to examine a Mach 2.3 separated SBLI to demonstrate the clear link between the reflected shock excursion and the size of the separation bubble, and detected the existence of coherent vortical structures in the separated shear (or mixing) layer.

They further analyzed the flow field in terms of convection of these coherent structures, which are easier to elucidate at lower shock intensities, and whose wavelength was measured between $0.2L$ and $0.4L$. Here they define the length scale, L pertinent to unsteadiness dynamics as the distance between the mean extrapolated positions of the reflected and incident shocks.

Subsequently, Piponnau *et al*⁶⁰ used simultaneous wall pressure and *PIV* measurements to develop pressure-velocity space-time correlations and combined these with linear stochastic estimation and *POD* techniques to predict the bubble motion. In another recent experimental study, Souverein *et al*³² varied the interaction strength at Mach 1.7 from weak (incipiently separated) to strong (fully separated) to examine features of unsteadiness. The large coherent structures downstream of the shock foot persist even in weak interactions where the separation bubble is highly intermittent and there is a higher correlation with the upstream region than in strongly separated cases. Their visualizations furthermore showed very clearly the existence of vortex shedding in the shear layer. They conclude that the dominance of different mechanisms may depend on the interaction strength, which in turn depends primarily on Mach number (usually a product with deflection angle, see glancing shock discussion in Ref. 61) rather than Reynolds number.

Although the possibility that facility dependence dominates unsteadiness has been discounted by the fact that multiple tunnels and simulations observe the same behavior, a major recent success is associated with the *HIFIRE-1* program. The test article, introduced earlier in Fig. 2(a), is comprised of a leading cone to study transition to turbulence, and a flare for *SBLI* – the two experiments are separated by a cylinder section. A tertiary experiment to test survivability of a mass capture measurement system (Tunable Diode Laser Absorption Spectroscopy, TDLAS) is also incorporated in channel cutouts on the flare. The detection of unsteadiness in the *SBLI* component permits two major conclusions: that the phenomena occur in flight and that they occur in axisymmetric situations, which have not been studied as much as the nominally 2-D cases. Kimmel *et al*⁶² show that high bandwidth pressure transducers on the *HIFIRE-1* flight test measure a bimodal distribution during ascent, which is “qualitatively similar to those measured in wind tunnel experiments”. These signals, with peaks in the range of 3kHz were obtained on a transducer located about 6cm upstream of the cylinder flare juncture (see Fig. 2(a) and zoomed shock structure in Fig. 3(c)), at a condition corresponding to a Mach number of 3.43 and well within the expected *SBLI* upstream influence for that point in the flight path.

Although many of the simulations, of *LES* and *DNS* level, have been performed at far lower Reynolds numbers than in experiment for computational expense reasons (cf. however Ref. 63), this factor has not been an impediment to their use for physics insights because of the relative insensitivity of the main features of unsteadiness to Reynolds number.³² Adams⁶⁴ examined a Mach 3 flow with an 18° compression ramp at $Re_\theta = 1685$. The simulations reproduced many of the expected behaviors, including amplification of turbulent kinetic energy, modification of structure parameter, and the failure of the strong Reynolds analogy in the interaction area, and the frequency of shock movement was “of similar magnitude to the bursting frequency of the incoming boundary layer”. One of the early detailed studies of low frequency unsteadiness was presented by Pirozzoli *et al*,⁶⁵ who used a Mach 2.25 impinging shock *DNS* to propose an acoustic-based resonance mechanism in which waves are generated by interaction of the incident shock with coherent structures. They developed a simplified model based on similarities to cavity flows and jet screech. Wu *et al*⁶⁶ also showed that simulations could reproduce the experimentally observed low frequency unsteadiness by considering a 24° compression corner.

A series of subsequent articles, a few of which are Refs. 67–72, played a very strong role in further elaborating on the dynamics, by using sophisticated statistical analyses to identify cause and effects. Only a few of these are discussed, since they provide the level of insight suited for this review article. Touber and Sandham^{69,70} examined different interaction strengths with *LES*. Their examination of the features of the interaction showed that instantaneous reversed velocities could be very large even in relatively weaker interactions. Their innovative efforts in using theory and simulation to propose underlying mechanisms are discussed further below.

Priebe and Martin⁷³ use low-pass filtering and spanwise averaging of *DNS* data to analyze in detail the motion of the shock and the shear layer formed at separation, which they note is different from canonical planar layers because of the existence of two inflection points at certain times. They connect their results to the likelihood of shear layer instability as the origin of the unsteadiness. In a more recent effort,⁷² they confirm the breathing of the bubble and associated flapping of the shear layer and further show that shock motion is more correlated to the downstream flow features (separation bubble and shear layer) than to the upstream boundary layer.

Agostini *et al*⁷⁴ use *LES* to explore the effect of interaction strength, from incipient to fully separated, in a Mach 2.3 impinging shock configuration with different generator angles, putting emphasis on the motion of the leading shock. Using correlations, they establish convection velocities of vortical structures in the mixing layer as a function of frequency to show that low frequencies do not have a convective component while intermediate frequencies do. They further separate the shock motion into components upstream and downstream of the crossing point and show their

connection to the kinematics of the vortical structures and the foot of the separation shock.

Several mechanisms have been proposed to explain the observations. As noted earlier, Ganapathisubramani *et al*⁵⁸ observed that the incoming upstream boundary layer entering the interaction had long (streamwise) structures which they subsequently connected to similar motions in incompressible flows.⁷⁵ These structures were also correlated to a waxing and waning of the boundary layer profile and could explain the unsteadiness since when the boundary layer was fuller/shallower, the shock moved downstream/upstream and further could also explain the observed spanwise variations because of their slender longitudinal character.

On the other hand, Refs. 76, 77 used their results to identify separation bubble dynamics including inherent instabilities of the shear layer, *i.e.*, downstream dependence, as the dominant aspect. They showed that a physical model based on vortex shedding and entrainment, essentially an oscillator type of description, predicts theoretical time scales for the bubble breathing, which match observations at multiple Mach numbers and interaction strengths. All results captured peaks in a narrow range of $0.025 < St_L < 0.04$, where $St_L = fL/U_\infty$. For reference, L varied depending on interaction strength from about 3.5 to 5.5 boundary layer thicknesses.

Touber and Sandham^{69,78} perturbed the *mean* flow obtained from *LES* with white noise to couch the dynamics in the context of a global mode to explain the broadband nature of the low frequency phenomena (this differs from the idea of local and global influence in Ref. 79). In a more recent article,⁷⁸ they examine results in the context of the theory of Plotkin⁸⁰ (see also Refs. 81, 82). The model essentially considers the shock motion as being described by a simple differential equation that includes a restoring force subjected to a turbulent forcing term. Based on a systematic derivation of the equation from the Navier-Stokes equations, Touber *et al*⁷⁸ conclude that the dynamics of the coupling can be represented as a first-order low pass filter and further that the “observed low-frequency unsteadiness in such interactions is not necessarily a property of the forcing, either from upstream or downstream of the shock, but an intrinsic property of the coupled system, whose response to white-noise forcing is in excellent agreement with actual spectra.” Recently, Poggie *et al*⁸³ present a comprehensive study that examines a range of ground test data, simulations and the *HIFiRE-1* data. Their analysis demonstrates that all these data fall within the amplifier type model construct of Plotkin⁸⁰ to conclude that “separation unsteadiness has common features across a broad range of compressible flows”.

As noted earlier, the experimental study of two-dimensional interactions has been plagued by the potential of three-dimensional effects associated with the sidewalls. Garnier⁴¹ computed the whole wind tunnel span of the *IUSTI* experiment¹² with Stimulated Detached Eddy Simulations to show that for strongly separated interactions, the centerline of the tunnel is contaminated with endwall effects. The patterns obtained are in many ways similar to more recent surface oil results of Titchner and Babinsky.⁴⁰ The description of such flows is greatly aided by the use of topological tools such as those described in Refs. 84–86. Some of the main effects observed in Refs. 40, 41 are topologically similar to those observed earlier by Zheltovodov⁸⁷ and simulated by Gaitonde *et al*.⁴⁷ The basic features are shown in Fig. 7, which represents the effect of the shock from the 15° fin of an asymmetric 7 × 15 double-fin configuration on the boundary layer associated with the 7° fin. Since the 7° fin is relatively small, the configuration represents only a minor modification from that of Refs. 40, 41, if reoriented by a 90° angle about the streamwise direction. Fig. 7(a) shows the experimental and computed surface patterns (with a modified RANS model as discussed in Ref. 47). In addition to the separation and attachment lines, the main topological feature is a focus similar to that observed in Refs. 40, 41. The corresponding flow field, shown in Fig. 7(b) with streamlines in addition to the surface pattern on the plate and sidewall, shows that the main feature is the ejection of the corner vortex due to the adverse pressure gradient. This pattern then smoothly asymptotes to the essentially 2-D separation region (Surface 1) far from the plate (corresponding to the 2-D center region of Refs. 40, 41).

The issue of contamination of 2-D with 3-D sidewall effects is somewhat moot in simulations, which can specify periodic boundary conditions, though it does raise the question of whether periodic conditions can truly represent the wind tunnel.⁴¹ Such issues, including whether a given spanwise size of the domain faithfully represents the flow, and the time of integration required to obtain accurate low frequency statistics have been explored in several publications. A particular area that remains of interest is the specification of the inflow condition representing an equilibrium upstream boundary layer. Since simulation of a transition process of the type that actually exists in wind tunnels is very difficult and computationally expensive, most researchers generate the incoming profile with artificial techniques, each of which requires care in its use and remains *ad hoc* to some degree. The fact that the Reynolds number is relatively small in simulations complicates the problem, since the development of turbulence is slower, regardless of technique used. Furthermore, each approach requires care in initialization *i.e.*, requires different levels of input conditions such as sample fluctuations or Reynolds stress distributions, which can dominate the efficiency of the method, making a relative comparison difficult.

Perhaps the most popular method is the recycling-rescaling procedure where the upstream boundary layer is initiated by a set of physics based perturbations, which are then evolved over a relatively short domain through recycling.

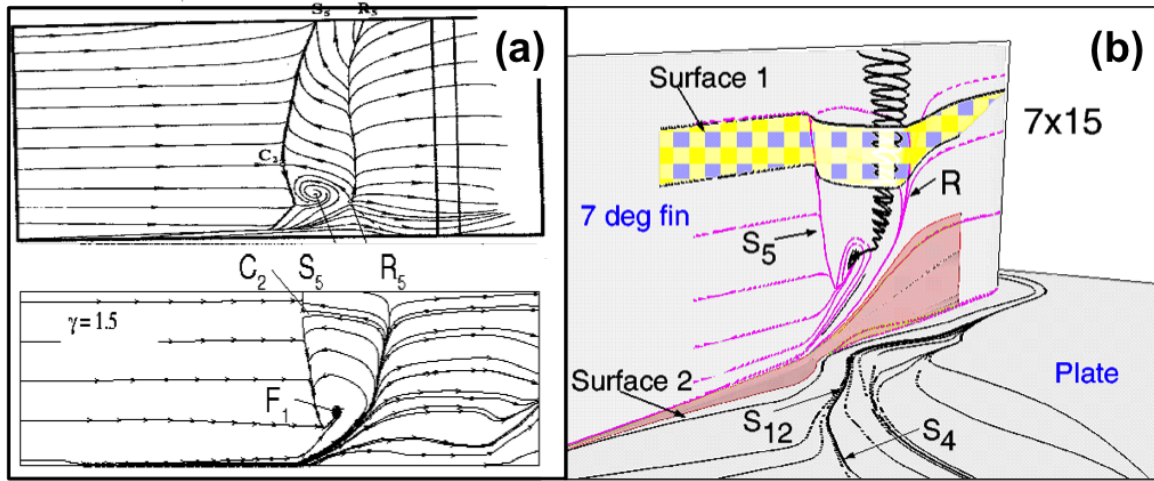


Figure 7. The effect of swept shocks on corner flows showing features similar to those observed due to 3-D contamination in nominally 2-D interactions (a) sidewall surface streamline pattern; (b) flow structure showing ejection of corner vortex

Issues with this approach include the need to address recycling of the inviscid wave structure, potentially spurious effects associated with a finite recycling domain and unphysical spanwise decorrelation. Detailed discussion of these issues and possible solutions have been discussed by Morgan *et al.*⁸⁸ who develop the dynamic reflection technique to minimize issues with spanwise correlations. The digital filter approach employed by Touber *et al.*⁶⁹ is seeing increased use.⁶⁷ The method requires initiation by mean flow and Reynolds-stress profiles which are seeded with suitable physically consistent perturbations based on filtered random numbers that are then allowed to relax. The relaxation process appears to depend on the conditions of interest and the closeness of the initial profile to the final desired conditions. Ref. 70 uses an approximately 25δ domain, at the end of which there remain perceptible undulations in C_f , while in Ref. 88, a shorter region of about 10δ is noted as sufficient for the same method. The method is very attractive, and further characterization in terms of multi-point correlations and parametric studies at different Mach numbers should yield valuable data on efficiency of the method.

Spatially evolving boundary layers by tripping mechanisms may be subdivided into two major approaches; an unsteady blowing suction technique used in, for example, Refs. 89, 90 and a more recently developed steady counterflow force based trip,⁹¹ which is a supersonic extension of the method of Visbal.⁹² The method was used to generate the interaction described earlier in Fig. 6. In this, an initial laminar boundary layer is subjected to a sharp retarding force that causes a small separated region, which in turn accelerates the process of transition to turbulence. Select highlights of the approach are shown in Fig. 8. Frame (a) shows the force field located a short distance downstream of a leading edge where a laminar incoming boundary layer profile is specified. Frame (b) shows the development of the spatially developing boundary layer in terms of coherent structures. Detailed analyses show that the obtained boundary layer has the correct mean, single and two-point statistics as well as anticipated coherent structures with no signature of the tripping mechanism (see Figs. 8(c), (d) and (e)). The method requires no special initial conditions other than a laminar compressible incoming boundary layer. As a method of upstream boundary layer generation, it is more expensive than the others - typically about $40 - 50\delta$ is required to obtain an equilibrium profile. However, the subsequent SBLI is performed on essentially the same mesh and a measure of efficiency is recovered. Current efforts are focused on making the process more efficient by determining the required force field for any Mach and Reynolds numbers with small computations focused on signatures in the recovering boundary layer near trip region.⁵⁵

Unsteadiness in genuinely 3-D configurations, such as the sharp or double fin, has been predominantly the domain of experiments, mostly performed until the late 1990s. Dolling and colleagues have examined numerous such configurations including swept corners, sharp fins, blunt fins and doublefins.^{28, 93-95} There has been relatively little effort in this area during the last decade however. Hou *et al.*⁹⁶ showed that the unsteadiness features upstream of a blunt fin had the same character as those upstream of a compression corner, even though separation scaled with different lengths for the two situations (cylinder diameter versus boundary layer height). The finding was correlated to the overall consideration that large scale events in the upstream boundary were the primary cause.

The distinction between 2-D flow and 3-D flows as discussed earlier in Section II highlights several key issues in translating the substantial progress in the former to the latter. For concreteness consider the flow past a fin on a plate. Since there is no reversed flow region in the mean sense (except for a very small region near the center of the channel – see Ref. 50) and is thus open (no recirculation). Convective aspects of the feedback mechanism are unlikely to be

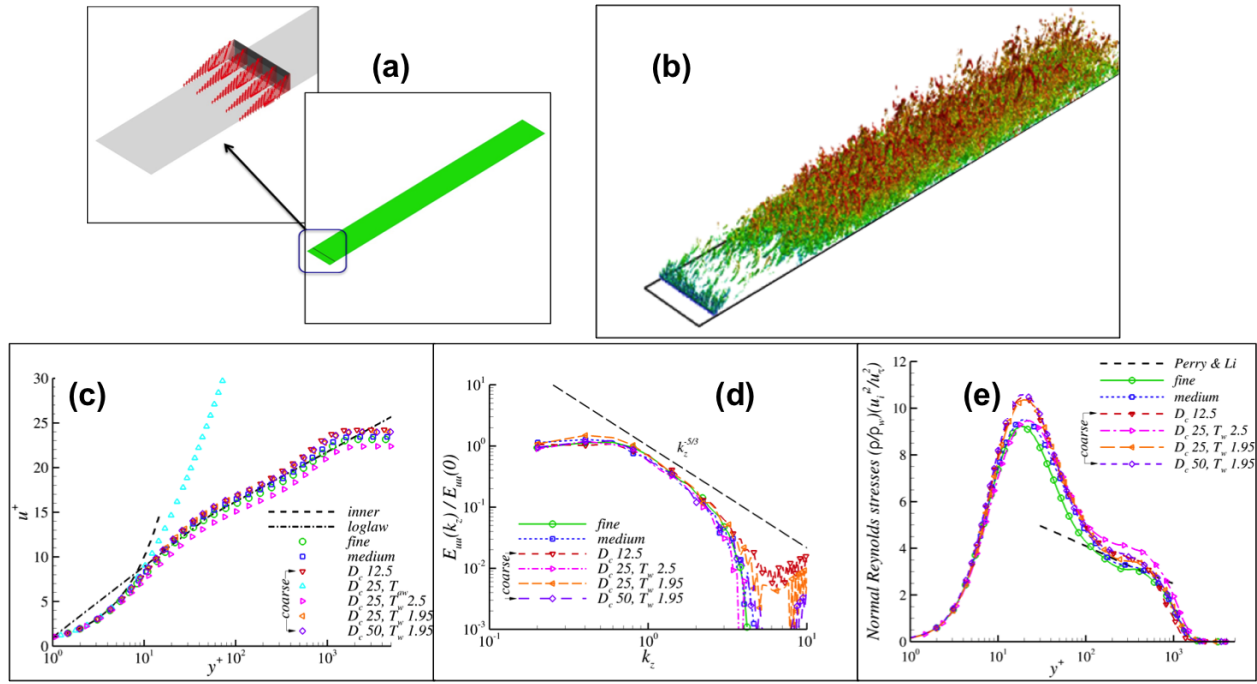


Figure 8. Counterflow actuator force method to obtain upstream boundary layer profile (a) schematic showing location of force; (b) development of coherent structures after transition; (c) law of the wall; (d) spectra in equilibrium region; (e) Reynolds stress variation. Different D_c levels indicate force strength

the same. Indeed, in a conical interaction, it is not possible to identify a unique separation length. For discussion purposes, we may tentatively identify this as the distance along a surface streamline from the line of attachment to the line of separation or perhaps the normal distance between the feet of the 3-D λ observed in such interactions (the downstream leg of the λ is quite diffuse). This length depends however, on the distance from the fin leading edge. The height of the boundary layer at the point of separation is also a function of spanwise distance. Thus, the length scale employed to normalize the frequency as in Ref. 77 may be variable. Furthermore, since the separated boundary layer does not reattach, its dynamics in terms of coherent structures likely have a different significance than in the 2-D situation.

In concluding this section, we mention that several studies have explored large scale unsteadiness, *i.e.*, where there is a substantial, often irreversible shock motion as in unstart or mode transition. These are discussed in the context of complex interactions, Section V.

IV. Heat transfer and skin friction coefficient

The last fifteen or so years have seen striking successes in heat transfer measurements and prediction in both ground and flight test. These studies have generally focused on axisymmetric configurations (without and with high-temperature effects), and considerable leverage has been brought to bear by combining international computational and experimental teams in the RTO/AVT framework. In this section, we first summarize results on activity until the turn of the last century, before discussing these more recent efforts.

Until the early 1990s, the problem of *turbulent* heat transfer rates was mainly the domain of experimental investigations. Parametric studies were performed by varying Mach (from transonic to hypersonic) and Reynolds numbers (10^5 to 10^7 based on boundary layer thickness) to generate comprehensive databases, including surface pressure, heat transfer and skin friction coefficient, which were then mined to obtain correlations. Expressions for peak heat transfer rates in several cononical situations for both laminar and turbulent situations may be found in Bushnell and Weinstein.⁹⁷ An extensive compilation of data and analysis for transitional and turbulent flows at different interaction strengths is presented in a series of publications by Holden *et al.*^{98–100} These consider a range of Mach and Reynolds numbers for attached and separated flows past flat plates, corners, curved compression surfaces, blunt leading edges, cone-flares, smooth and rough hemispherical nose shapes, biconic nosetips with different roughness patterns and shock/shock interactions (discussed further below). The measurements include pressure, skin friction coefficients, heat transfer rates, force and moment values. These efforts were designed to understand the practical implications of various parameters and also to examine the data in the context of the hypersonic interaction parameter, Reynolds analogy factors, available

semi-empirical theories such as those of van Driest¹⁰¹ and Eckert¹⁰² and to serve as databases for *CFD* validation. One limitation however is that these have been mostly steady data, a general deficiency that was also noted in the 2001 review by Dolling,¹⁰ and which persists today.

In the mid-1990s, more experimental efforts actively considered data generation and processing for numerical validation. An early example for the types of canonical configurations shown in Fig.1 is the compendium of nineteen “professional quality” measurements assembled in Ref. 13. The standards chosen were that the data be turbulent, on relatively simple geometries (*i.e.*, not on demonstration type test articles), applicable in the sense that they are good enough to explore turbulence modeling (typically requiring measurements of multiple variables, including heat transfer), had clearly noted experimental boundary conditions and error bounds, were self-consistent and adequately resolved. Other efforts include a particularly detailed and systematic set of measurements, including surface pressure, heat transfer, skin friction and field Pitot surveys, at Mach 8.3 on impinging shock, single-fin and double fin interactions by Kussoy *et al.*^{14,44} Similarly, Garrison *et al*^{48,103} publish skin friction coefficient results for the double fin.

These data have been extensively used by computationalists to predict surface quantities by examining turbulence modeling aspects: several examples were presented earlier in Fig.4. Knight and Degrez⁸ compile *RANS* results from simulations for several 2-D and 3-D interactions. The models range from algebraic to full Reynolds Stress Equation formulations for the single fin, double fin and the hollow cylinder flare. The basic conclusions were that heat transfer and skin friction predictions were “generally poor”, with up to 100% discrepancy for the stronger interactions displaying significant separated regions.

For complex hypersonic laminar interactions however, the last decade has seen a very systematic, substantial and successful effort to document and demonstrate measurement and simulation accuracy. This reflects the explicit recognition that *CFD* development required *CFD* friendly experiments with careful specification of freestream and boundary conditions. High quality data including pressure and heat transfer were obtained at different Mach and Reynolds numbers for the hollow cylinder flare and double-cone (or “biconic body”).^{37,104} These interactions are of the type that can be considered “building block”,¹⁰⁴ *i.e.*, canonical in a geometric sense, yet manifest shock-shock and shock-boundary layer phenomena that result in an order of magnitude enhancement in heat transfer rates. Furthermore, axisymmetric situations obviate the difficulties associated with 3-D contamination that plague nominally 2-D interactions. These new databases are a natural progression of data discussed in Refs. 99, 100. Several nitrogen and air flows are at enthalpies large enough to engender significant high temperature effects, which facilitates exploration of chemistry models.

Reference 37 documents blind validation results on cold flows, *i.e.*, with no significant high-temperature effects, using a wide swath of numerical methods for cylinder-flare and cone-cone interactions in the Mach 9 to 12 range as part of AFOSR and RTO/AVT activity. The results, including some with low-density effects, were compared on the basis of several quantitative metrics, including separation point, pressure coefficient C_p and Stanton number, St . Solutions were presented by several groups of researchers, including Candler *et al.*¹⁰⁵ Gnoffo,¹⁰⁶ Kato and Tannehill,¹⁰⁷ Moss,¹⁰⁸ Boyd,¹⁰⁹ D’Ambrosio¹¹⁰ and Gaitonde.³⁵ The discussion in Ref. 37 indicates that for flows known to be laminar, the overall success could be deemed “impressive”. Key aspects of the two flows were accurately reproduced by most of the methods and decisions on parameters inherent in numerical approaches could be made “blindly”. As an example of the level of agreement, Figures 9(a) and (b), taken from Ref. 35 exhibits pressure and heat transfer rates for Run 28 of Ref. 37, corresponding to a freestream Mach number of 9.59 and Reynolds number of $1.4 \times 10^6/m$. The grid converged results are clearly reasonably accurate for both pressure and heat transfer rates, as well as extent of the separated region. The discrepancy in the initial heat transfer rate prior to separation has been thought to be associated with differences in characterization of the freestream conditions due to vibrational freezing in the nozzle.

The success of this systematic joint experimental computational effort for laminar, relatively cold hypervelocity flows encouraged the extension to flows with high-temperature effects. This is a considerably more difficult endeavor, since issues such as proper characterization of the freestream, and conditions on the surface (catalycity) are often not known. Nonetheless, a series of papers in the mid 2000s clearly shows substantial and systematic progress (see *e.g.*, Refs.104, 111–114). Ref. 115 summarizes some of the key findings *circa* 2008, noting deficiencies in real gas chemistry and surface condition characterizations.

Another comprehensive effort, again with teams working under the umbrella of AFOSR and RTO/AVT programs culminated in a series of simulations, with high-temperature effects, which are summarized in a review article by Knight *et al.*¹¹⁶ Figure 9(c) and (d), taken from Ref. 117, shows sample results for Run 42 (Nitrogen flow at Mach 11.6 at $9.17 MJ/kg$ enthalpy). Although vibrational relaxation is important in this flow, it is evident that chemistry models developed until 1990s provide a reasonable estimate of the main parameters of interest. The other major case examined in this set of tests is the flow of air past a cylinder based on experiments performed at DLR,¹¹⁸ where

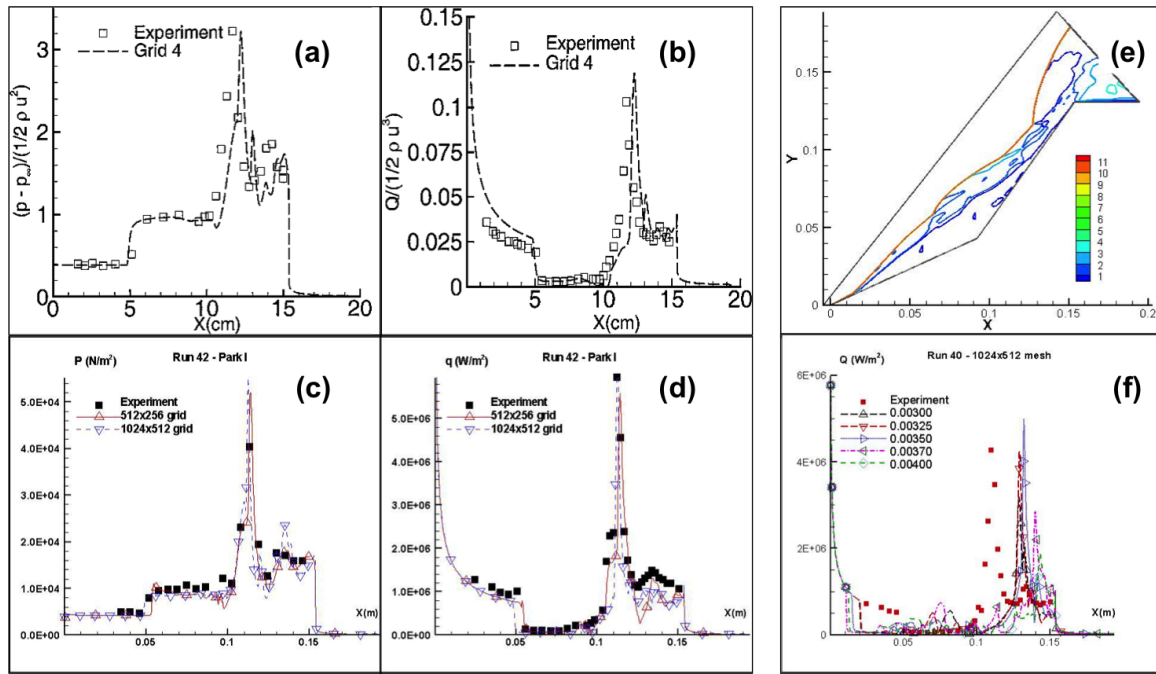


Figure 9. Sample results on double cone configurations. (a) and (b) pressure and heat transfer rates in cold flow; (c) and (d) pressure and heat transfer rates in flow with high-temperature effects; (e) instantaneous Mach number contours of non-convergent case; (f) evolution of heat transfer rates for non-convergent case

scatter was evident between different chemistry models and significant sensitivity was observed to surface catalycity assumptions. Issues for future research therefore include air chemistry effects at very high enthalpies and gas surface interactions.

Although a corresponding systematic examination of simulation capability in reproducing turbulent heat transfer rates with *DNS* or *LES* has not been performed, substantial progress has been made in the last decade in more practical contexts, with *RANS* and hybrid *RANS/LES* methods. *RANS* methods have leveraged understanding of shock-turbulence interactions to generate workable model modifications in 2-D by accounting for different phenomena such as compressibility, streamline curvature, effect of adverse pressure gradients, turbulence amplification through shocks and reattachment (see *e.g.*, Refs. 119–121).

A few recent efforts to characterize the accuracy (uncertainty quantification) of *RANS* in *STBLI* are now summarized. Roy *et al*¹²² compile an exhaustive database of experiments and use several to review and assess a wide range of turbulence models for compression corners, cylinder flares, cone-cones and 2-D and axisymmetric impinging shocks. They make several specific recommendations for future experimental campaigns regarding uncertainty characterization. DeBonis *et al*¹²³ also review the efforts of several researchers using different models to reproduce experiments from *IUSTI* and University of Michigan. They examine velocity and Reynolds stress profiles in an uncertainty quantification based framework to conclude that the performance of the turbulence model depends on the quantity employed to assess it, with some models performing well for one quantity but not for the others. Grid type (unstructured versus structured) did not have significant influence.

Earlier this year, Bose *et al*¹²⁴ introduce a special section of the Journal of Spacecraft and Rockets to examine “uncertainties in predictions of heat flux and pressure in hypersonic flight using state-of-the-art aerothermodynamics codes”. Of the four problems of interest, two involve *SBLI*, those due to compression corners and impinging shocks. Results including heat transfer rate comparison with data obtained mainly from CUBRC and NASA are presented by Gnoffo *et al*¹²⁵ and Brown,¹²⁶ respectively at mission-relevant conditions and include high-temperature effects for the compression corner. These papers carefully describe the different modifications employed in each turbulence model used and then introduce systematic criteria to assess uncertainty and accuracy. They successfully highlight the difficulty in performing careful assessment, since codes typically have multiple components, including the turbulence model, discretization techniques for viscous and inviscid terms, limiters *etc.* They also identify the need for more experimental data, and certainly availability of data of the quality and breadth described above for laminar interactions would greatly aid further development of turbulent flow simulation capability.

The *HIFIRE-1* test, which was earlier discussed in the context of low frequency unsteadiness, has generated a wealth of pressure and heat transfer data on flare-induced *SBLI* from ground^{127, 128} and flight campaigns.²¹ These data

have been employed in numerical efforts both to evaluate CFD tool capability as well as to understand the overall flow structure. Wadhams *et al*¹²⁷ and MacLean *et al*¹²⁹ describe an impressive joint experimental and computational study with the ground test campaign at CUBRC. Their results indicate the manner in which RANS could be used to analyze such data through systematic evaluation of modeling terms based on an understanding of flow processes.

For flight test data, an extensive computational study has recently been performed by Yentsch *et al*^{34,130} to examine three points on the ascent trajectory (5, 15 and 20 seconds, corresponding to Mach 2.85, 2.63 and 5.09 respectively). Fig. 10(a) and (b) show the flow structure near the flare. Frame (a) is essentially the same as that shown earlier in Fig.3 but including the channel cutout. The overall flow field is very complex, especially near and inside the channel. The streamlines, Fig. 10, show the manner in which the separated flare flow interacts smoothly with the relief associated with the channel. Features due to the ramp in the channel and its corner can be discerned,³⁴ including the presence of lip vortices generated at the channel edges. The mean line of separation shows slight non-uniformity near the channel, but overall, the axisymmetric assumption appears reasonable at 90° to the channel, which did not contaminate the SBLI experiment. The performance of a popular $k - \omega$ model variant¹²¹ was found to be dependent on the flow condition. Although low heat transfer rates and data scatter complicated heat transfer comparisons at $t = 15s$, results at the highest Mach number, $t = 20s$, indicate relatively better agreement as shown in Figs. 10(c) and (d) respectively. Note that the effect of the impingement near the shoulder results in heat transfer rates that are over 8 times higher than upstream of the interaction.

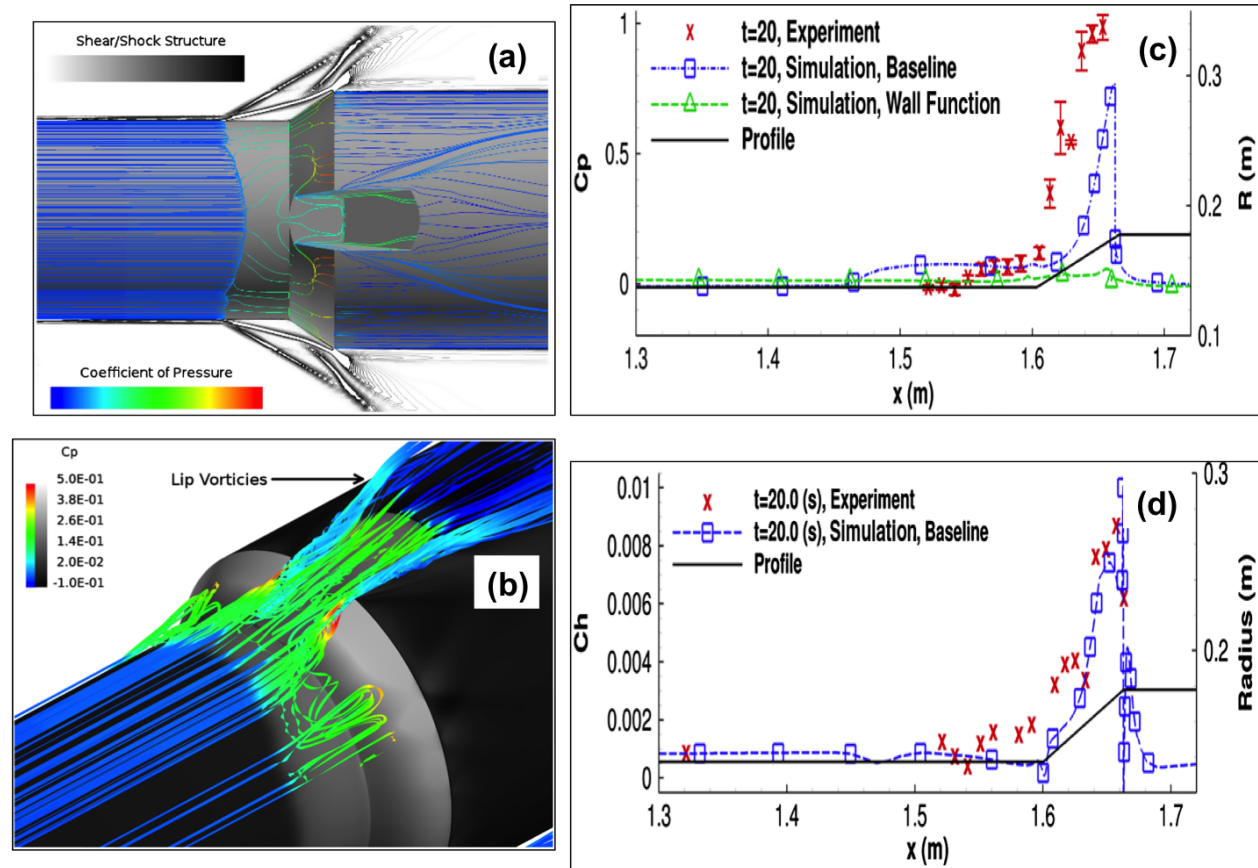


Figure 10. Computational and experimental results from the HIFIRe-I flight test. (a) shock structure and surface streamline visualization; (b) streamlines near flare and channel cutout; (c) pressure coefficient near flare region; (d) heat transfer coefficient near flare region

A promising development over the last several years has been of hybrid methods. In contrast to the DES approaches, which switch from RANS to LES in separated flows away from walls, hybrid methods also treat attached flows, reducing the required computational resources with tailored near-wall RANS blended with LES away from the surface. A series of publications by Edwards *et al* describes the evolution of the procedure for different types of flows, including SBLI.¹³¹⁻¹³⁴ The corresponding required extension to the upstream profile generation approach based on recycling-rescaling is presented in Ref. 135. Sample results on 2-D (compression corner at Mach 5) and 3-D (double fin at Mach 8.3) configurations with significant separation may be found in Refs. 136, 137 and 138 respectively. The results are striking particularly for the more examined nominally 2-D case in that both the mean and unsteady aspects of the flow – including low frequency phenomena and power spectra – are reproduced fairly well and the separation

front correlates with streaks in the flow. The results also detect counter-rotating vortices in the mean flow thought to be associated with Goertler instabilities.

The use of *DNS* or *LES* to connect heating rates to turbulence structure in *SBLI* requires some consideration of Reynolds number. Whereas there is evidence that low frequency unsteadiness is not particularly influenced by Reynolds number, the dependence of heat transfer rates on this parameter requires careful thought. The need for quantitative accuracy may require evaluation at higher Reynolds numbers that are currently outside the reach of *DNS* and *LES*. Nonetheless, some of the basic qualitative dynamics, in terms of coherent structures and their impact on establishment of heat transfer rates may be possible with simulations at lower Reynolds numbers. High quality unsteady experimental data will however be required. We note however that sometimes simulations at parameters where the experiment is laminar may for numerical reasons generate results that indicate transitional or turbulent flows. For example, in Ref. 117 it is shown that simulations do not converge for Run 40 from the CUBRC database. Aspects of this anomalous behavior are shown in Figure 9(e) and (f). Although the shock system sets up correctly initially, as the solution is marched forward, it then continues to evolve until the upstream influence of the flare approaches the cone tip. The separated region increases and peak heat transfer rates diminish and move downstream until they reach the shoulder of the second cone. A similar observation was made by the author for the cold case designated Run 24 in Ref. 37. One possibility for this observation is based on the fact that these cases represent relatively higher Reynolds numbers in the datasets. If the simulation, whether for physics-based or numerical reasons, predicts them to be transitional or turbulent, then approaches based on axisymmetric assumptions cannot reproduce the dynamics (absent a turbulence model), and *LES* or *DNS* are necessary (calibrated *RANS* being perhaps acceptable for engineering purposes). This has implications to the cost of simulation. Although the spanwise domain width required for nominally 2-D interactions is relatively well characterized (roughly 2 to 5δ appears sufficient), an equivalent requirement for the axisymmetric situation remains unknown. Since the boundary layer thickness is usually a small fraction of the cross-sectional diameter of the axisymmetric body, if it turns out that the entire azimuthal domain needs to be simulated, then axisymmetric situations may be more expensive than nominally 2-D ones.

Other than the hybrid *RANS/LES* efforts described above, there have been relatively few examinations of 3-D canonical configurations such as the single or double fin configurations, since the work of Ref. 8. Thivet *et al*¹³⁹ employ the basic flow model shown earlier in Fig. 5 to analyze in detail the performance of the $k - \omega$ model and, by enforcing realizability constraints, manage to reduce the error in predictions along the centerline. However, as observed in Fig. 5, the centerline in some ways is an anomaly since it is straddled by small centerline vortices. The dominant part of the plate downstream of the separated boundary layer is in fact influenced by the flow that attaches near the corner and has a large spanwise velocity component. Consider for example, the flow that essentially originates downstream of the line of attachment that forms near the fin-plate corner. Figure 11(a), taken from Ref. 45 depicts the pressure gradient (left) and static pressure (right) on either side of the line of symmetry on a cross-flow plane. A select

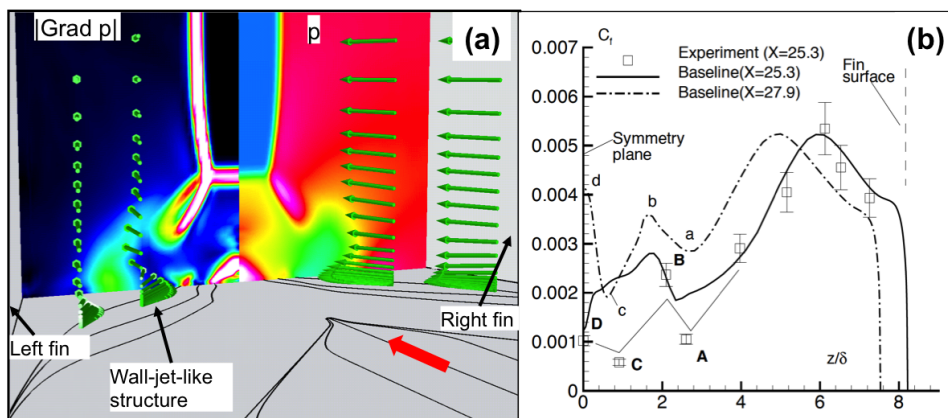


Figure 11. Correlation between shock, streamline structure and skin friction coefficient. (a) 3-D view of flow with wall-jet-like feature; (b) skin friction coefficient at different stations as compared to experiment

set of 3D velocity vectors is superposed. A careful examination of Figures 5 and 11 reveals that fluid in the entrainment regime after attachment, constitutes a “new” boundary layer, subjected to a favorable pressure gradient and develops a wall-jet like structure that is quite different from the phenomena near the centerline. Indeed, its state could be laminar, transitional or turbulent and needs further exploration. Depending on circumstance, correlations based on Reynolds analogy or simplified analysis for boundary layer flows may become appropriate even in this complex situation. We note that the good agreement with surface skin friction lines and the oil flow patterns (see Fig. 4) indicates that the trends in C_f should be reproduced accurately, and such is indeed the case. The skin friction coefficient variation along

the cross flow, shown in Fig. 11(b) indicates consistency with the surface oil flow (Fig. 4) and experiments of Garrison *et al.*⁴⁸ As discussed extensively in Ref. 47, insight can be obtained if it is recognized that the simulations reproduce many key features observed in experiment, but they may be displaced relative to their location in experiment.

V. SBLI in complex configurations

Ramjet and scramjet flowpaths are comprised of several regions where *SBLI* are important. Mixed compression inlets and isolators exhibit a series of such interactions at different Mach numbers and boundary layer thicknesses. Figure 12 shows some of the pertinent features in rectangular and circular cross-section devices. *SBLI* in the inlet regions generate separated flow in both configurations. The canonical double fin configuration of Fig.1(f) discussed earlier in the context of Figs.4 and 5 is highly pertinent in this regard: the main feature downstream is the low energy mushroom shaped region whose genesis is similar to that shown earlier in Fig.4(c). There are many other features that arise in such flows on sidewalls and in corners, interactions with injection jets, flame devices and so on, whose description may be found for example in Refs. 140–146.

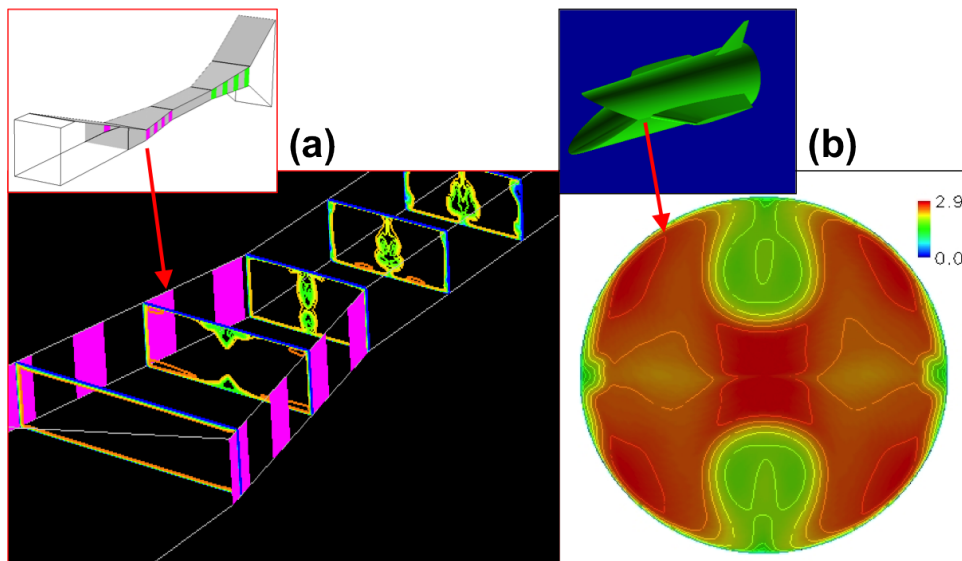


Figure 12. Internal flows in propulsion systems: (a) rectangular cross-section flow path; (b) circular cross-section flowpath (Jaws configuration)

Complex multiple *SBLI* such as those occurring in isolators have been explored in the context of unstart by Clemens *et al.*^{141,147} They describe a series of experiments performed under an AFOSR MURI on the unstart processes in an inlet/isolator at Mach 5. The sequence of large scale unsteadiness is initiated by flap deflection and observing the shock system with an array of diagnostics, including schlieren imaging, fast-response wall pressures and *PIV*. Their observations describe changes in the speed of the shock, which varies significantly from moderate to low to high in the 35m/s to 74m/s range, as it moves upstream. After unstart, a buzz like phenomenon at two possible frequencies (124Hz or 84Hz) with high and low pressure fluctuations respectively is observed. The concomitant separation regions, noted to be large, highly three-dimensional and unsteady, correlate with the largest adverse pressure gradients. The results have been employed to detect and model transient dynamics of unstart.^{140,148}

As noted in the motivation, although not a specific focus of interest, *SBLI* are a major factor, with well recognized impacts, in practical systems such as the *HIFiRE-2* and *X-51* programs. The *HIFiRE-2*²³ program, introduced in Fig.2(b), has been especially helpful from the basic research perspective because of the ready availability of ground-test data, key parameters such as flight profile, test conditions and geometric configuration. Briefly, the forebody inlet is designed to reduce spillage and to facilitate both dual-mode and scramjet operation as the rocket accelerates from Mach 5 through 8. A heavy fuel surrogate ethylene methane mixture is employed to facilitate burning in a relatively short flow path with a cavity flame holder. Unconventional side exhaust nozzles are employed to allow the payload to be coupled to the sounding rocket stack booster, which remains attached to provide thrust for the payload throughout the captive flight test. Some of the main ground test data, performed at the NASA Langley Arc-Heated Scramjet Test Facility, may be found in Refs. 24, 149: although these do not account for *SBLI* in the inlet and isolator regions, their use in validating and anchoring CFD has been invaluable (see *e.g.*, Refs. 150–153).

A recent effort by Yentsch *et al.*¹⁴² examines the effect of the inlet by first anchoring results to the ground tests^{24,149}

and then leveraging the proven model to analyze the flight test. Figures 13(a) and (b) show the shock patterns in ground test and flight for the dual-mode case. The effect of the inlet distortion is evident in the overall shock structure: note the difference in location and shape of the normal shock. Figure 13(c) and (d) compare experimental tare (no combustion) and combusting C_p values to simulations using the $k - \omega$ model and the Taitech-Princeton 2 model (see Ref. 142 for details). Although there are several areas where the comparison may be improved, the simulations reproduce the main elements in the inlet as well as the pressure rise associated with combustion. Overall, the results indicate that *SBLI* due to the inlet influence the flow upstream of the combustor, and significantly change quantitative details in the flowpath, but that the dominant effects for this configuration are similar to those obtained in direct connect ground test facilities.

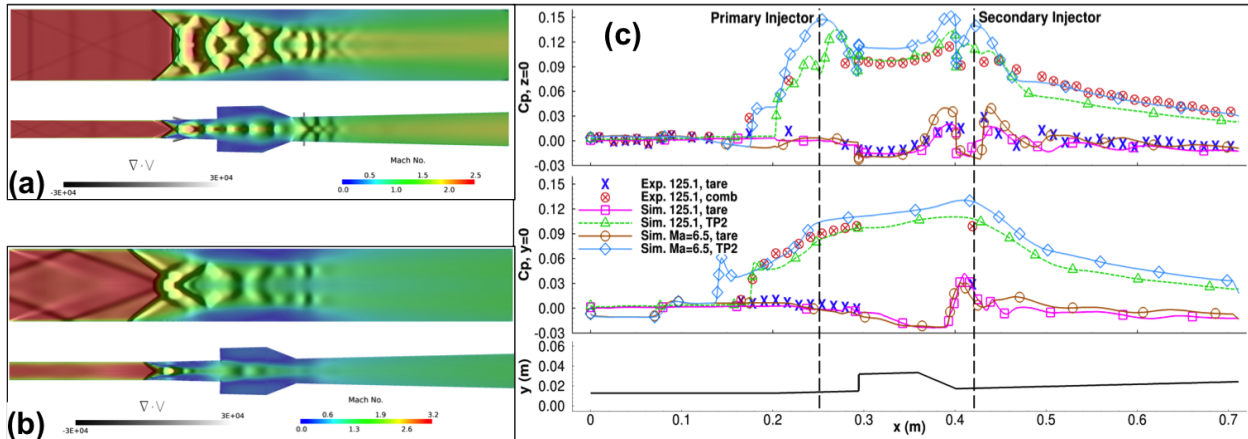


Figure 13. Computational and experimental results for the HIFiRE-2 configuration. (a) computed shock structure in ground test condition; (b) computed shock structure in flight test condition; (c) comparison of C_p on vertical and horizontal symmetry plane surfaces with ground test

Several other ongoing efforts have relevance to the effect of *SBLI* in complex configurations. Ref. 154 describes facility details in preparation for testing the HIFiRE-2 configuration in ground test. Diagnostic tool development is also progressing rapidly in various areas: for example, Ref. 155 elaborate on shock structure visualization in a scramjet flowpath, while Refs. 146, 156 discuss development of the non-intrusive TDLAS, which has the potential to greatly aid in the identification of shock motion, especially those that may herald imminent unstart.

VI. Control

The traditional approach for *SBLI* control has centered around mass transfer. Bleed is frequently employed to alter the properties of the boundary layer, for example reducing its shape factor thus making it more robust to adverse pressure gradients, while blowing and transpiration are considerations for cooling purposes. The basic considerations in the use of mass transfer have been discussed in Ref. 4, which summarizes several issues such as optimal regions including location, distribution and inclination of holes or porosity. Simulation on a 3-D interaction due to a sharp fin with bleed and zero mass flux techniques may be found in Refs. 157 and 158 respectively.

The recent decade has seen the development and application of several passive and active methods. Ref. 159 discuss the use of Mesoflaps for Aeroelastic Recirculating Transpiration (MARTs), which use variable deformation aeroelastic flaps to exploit pressure differentials at different locations to induce advantageous recirculation. Experimental results indicate that certain arrays of such devices could yield significant improvements in pressure recovery of a normal shock interaction. Ghosh *et al*¹³⁴ simulate this flow using an immersed boundary method and RANS and hybrid RANS/LES models. Their results suggest that for the configuration tested, there is a possibility of a connection between the dominant frequency of the flap and the low frequency shock motion and further that the axial separation is not substantially influenced by the control system.

Streamwise slots have also been shown to yield a degree of control authority as discussed in Ref. 160. The effect of these essentially 3-D devices, *i.e.*, segmented in the spanwise direction, was shown to have a “global control effect and lead to reduced stagnation pressure loss,” with the original 2-D separation bubble being divided into “highly three-dimensional regions of attached and separated flows.” Bumps have also been employed to generate similar effects: in Ref. 161, different configurations were evaluated to essentially break up the 2-D separation region associated with a normal shock interaction by generating streamwise vortex pairs. The use of protuberances (microramps¹⁶² or micro vortex generators) to generate such vortices to enhance entrainment and mixing has also been discussed in a

recent effort by Lee *et al.*¹⁶³ The effectiveness was shown to be higher at lower Mach numbers (1.4) than at higher values (3.0), a fact that was correlated to faster decay of streamwise vorticity and turbulent kinetic energy at higher speeds. Comparisons of different passive concepts have also been tested: for example, Ref. 164 assesses bleed versus micro-vortex generators on boundary layers by examining their effects on the shape parameter and skin friction. The effectiveness of combinations of bleed and vortex generators to address the corner flow and the central nominal 2-D *SBLI* has been presented in Ref. 40. The results appear to indicate that the use of vortex generators is potentially helpful if the flow is truly nominally two-dimensional.

The emphasis in recent years has shifted to active flow control. Microjets¹⁶⁵ have recently been used by Ali *et al*¹⁶⁶ to explore *SBLI* control. The steady jets, placed upstream of a 24° compression ramp at Mach 2, generated supersonic cross flow, which effectively muted the separation shock with significant reduction in the mean pressure downstream of the separation shock (7%) and on the ramp surface (25%) and accompanying reduction in unsteadiness. Verma *et al*¹⁶⁷ focus on amplitude of shock unsteadiness in the same interaction, with jets placed 12.5δ upstream of the corner in two different configurations, number and orientation of the devices. The results depend on the specific arrangement as well as the jet stagnation pressure, but up to 67% reduction in peak rms value was observed with certain settings.

The substantial success in understanding and analyzing low frequency unsteadiness, observed to be in the $O(1kHz)$ range, and thus accessible to several devices of adequate bandwidth, has triggered renewed interest in instability manipulation. Plasma-based devices have been of particular interest. In a series of studies, Webb *et al*^{56,57,168} use Localized Arc Filament Plasma Actuators (LAFPAs) to examine control of an impinging shock *SBLI*. They placed these devices, which use a very small amount of energy relative to that of the flow, upstream of the interaction, with the intention of exciting instabilities in the separated shear layers. The results indicated that the primary effect of the actuators was similar to that of heating *i.e.*, there was no significant amplification effect associated with instability manipulation, and the results were similar to those observed with wall heating in Ref. 169. Mullenix *et al*⁵⁵ examined the problem computationally by placing the actuators at the same locations as those of the experiments *i.e.*, upstream of the interaction ($x/\delta = 52.6$) (see Fig. 14(a)), but by exciting them at $St = 0.5$, representing the peak frequency inside the separated region, rather than the local peak $St \sim 0.03$. The model for the actuators has previously been shown to be successful in the analysis of flow control of a Mach 1.3 jet. The mean C_f values, Fig. 14(b), show a modest effect on the separation point, as well as on the profile inside the separation bubble, where a partial recovery is observed. The mean separated region is estimated to be reduced by 10%, though the analysis has not focused on whether there is any effect on the flow instability. Figures 14(c) and (d) show velocity profiles at several locations upstream and into the interaction. The results indicate that the velocity profile is affected substantially in the regions immediately downstream of the actuator location ($x/\delta \sim 53.6$ and 54.6) but relaxes back to the uncontrolled values further downstream. In other experiments, Nishihara *et al*¹⁷⁰ perturbed compression corner generated shocks with nanosecond pulsed dielectric barrier discharge (NS-DBD) actuators. Using phase-locked schlieren images and Laser Differential Interferometry (LDI) spectra, they demonstrated a degree of control authority in moving the shock and altering the low frequency oscillation characteristics.

Bisek *et al*¹⁷¹ examine control of Mach 2.25 flow past a 24 deg ramp with a magnetically-driven surface-discharge actuator based on experiments performed at Princeton University. Steady control without and with Joule heating and pulsed control at $St = 0.28$ with duty cycle of 50% were examined. The results suggest that the steady control case yielded the largest reduction in separation length (75%), low frequency content and amplitude of the turbulent kinetic energy in the separated region and downstream of attachment respectively. Other magnetohydrodynamic based methods for *SBLI* control have been discussed in Ref. 172 which exploits 3-D relationships between the magnetic and electric field and velocity vectors to propose an eddy current based method to suppresses secondary separation in the double-fin configuration. Leonov *et al*¹⁷³ and Bobashev *et al*¹⁷⁴ discuss numerous experimental results documenting the use of *MHD* on inlet associated shocks.

Finally, pulsed plasma-jet actuators have been tested for *SBLI* control.^{175,176} These devices, with demonstrated capability of up to 4kHz frequency, essentially use a spark in a cavity inside the plate to generate a jet which is then ejected into the flow. A parametric study¹⁷⁶ indicates that for a Mach 3 flow past a 20° compression ramp, jets angled 20° from the wall and pulsed at 3.2kHz reduced the “size of an approximate measure of the separation region by up to 40% and increased the momentum of the downstream reattached boundary layer.” The optimal placement was observed to be 1.5δ upstream of the corner. The effect appears to be a combination of both momentum injection and streamwise vortex generation.

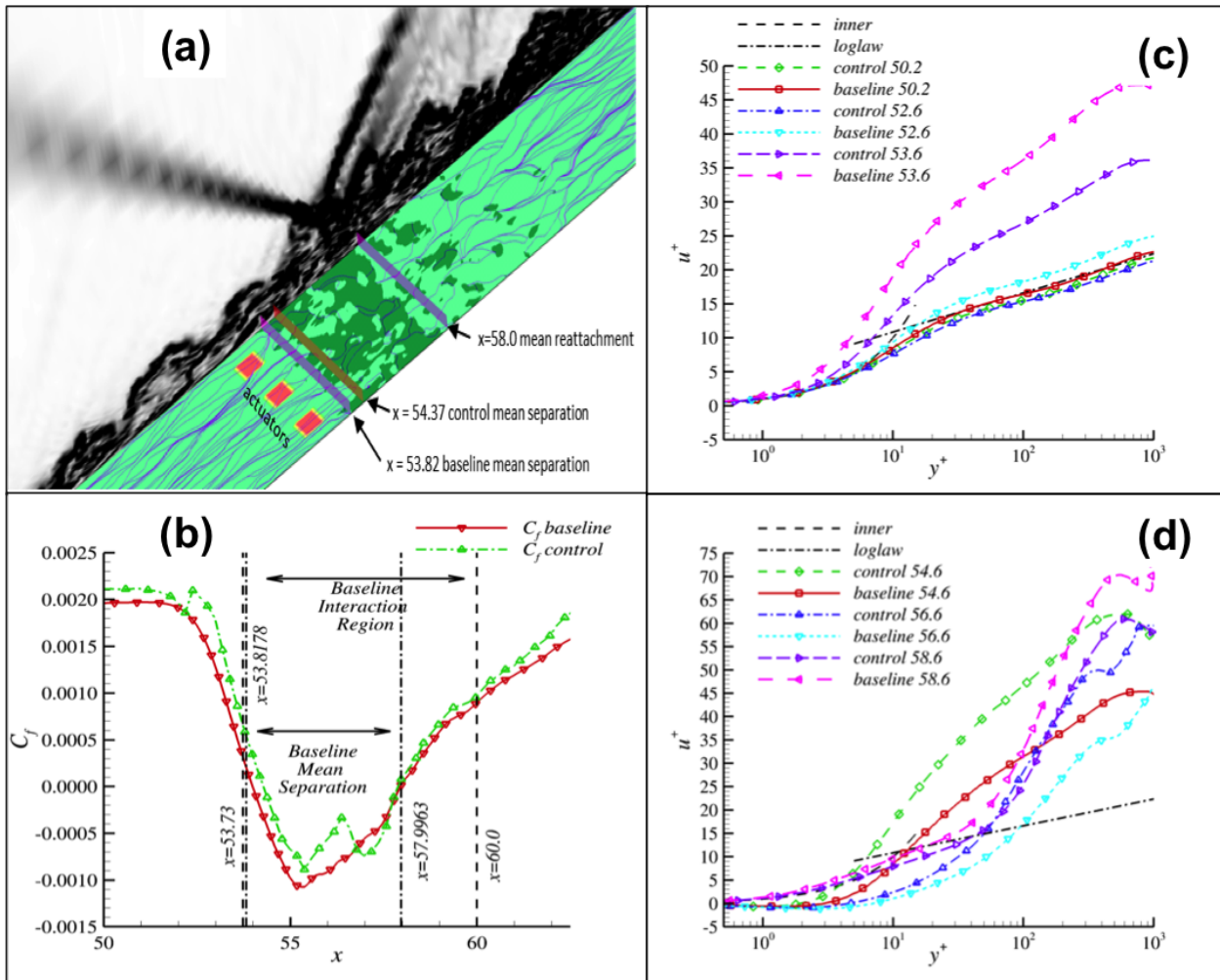


Figure 14. LAFPA control of *SBLI* interaction. (a) overview of actuator location and results; (b) skin friction variation; (c) and (d) velocity profiles at different locations in the interaction

VII. Conclusion

Recent activity in *SBLI* and its control over the past several years has been summarized with emphasis on the conclusions derived by various researchers together with some insights into outstanding issues. Breakthrough progress has been achieved in predicting and understanding the problem of low frequency unsteadiness in nominally 2-D interactions. This success has been achieved through complementary experimental and numerical analyses, which have identified the main phenomenology and integrated these into fluid dynamics models that provide insight into the main driving mechanisms. Control techniques based on this understanding have been attempted but may be considered to be in their infancy. Heat transfer rates measurement and prediction capability have also seen progress. For axisymmetric laminar flows without and with high temperature effects, there appears to be fair success at reproducing even very complex phenomena at moderate enthalpies. The uncertainty in turbulent heat transfer rates using RANS on nominally 2-D situations has been quantified as a take-off point for accuracy enhancements. The 3-D situation has not been examined in as much detail, though hybrid RANS/LES methods have shown promising results. The acquisition and continuing analysis of carefully characterized flight and parallel ground test data is an exciting development that will greatly determine future research direction.

Acknowledgement

The author wishes to acknowledge extended discussions on *SBLI* with several colleagues, within and outside the context of this paper. The author is grateful to J. Poggie and M. Visbal, who respectively clarified the distinctions between different unsteadiness mechanisms and their implications in 3-D separated flows. Other individuals whose

insights have benefited the author include F. Alvi, N. Bisek, M. Brown, G. Candler, M. Choudhari, N. Clemens, J. Dunbar, J. Edwards, M. Gruber, M. Hagenmaier, R. Kimmel, M. Holden, J. Schmisseur, M. Samimy and J. Shang. The author has used schematics provided by F. Alvi and N. Webb and is especially grateful to Robert Yentsch for his assistance. The simulations described were performed with a grant of computer time from the DoD HPCMP and the Ohio Supercomputer Center. The research was sponsored by AFOSR (monitor: J. Schmisseur).

References

- ¹J.E. Green. Interactions between shock waves and turbulent boundary layers. *Prog. Aero. Sciences*, 11:235–340, 1970.
- ²J.D. Schmisseur and P. Erbland. Introduction: Assessment of aerothermodynamic flight prediction tools through ground and flight experimentation. *Progress in Aerospace Sciences*, 48–49:2–7, 2012.
- ³R. Korkei. Survey of viscous interactions associated with high mach number flight. *AIAA J.*, 9(5):771–784, 1971.
- ⁴J.M. Delery. Shock Wave/Turbulent Boundary Layer Interaction and its Control. *Prog. Aerospace Sci.*, 22:209–280, 1985.
- ⁵A.G. Panaras. Review of the Physics of Swept-Shock/Boundary Layer Interactions. *Prog. Aerospace Sci.*, 31:173–244, 1995.
- ⁶A. J. Smits and J.P. Dussauge. *Turbulent shear layers in supersonic flow*. AIP Press, 1996.
- ⁷G.S. Settles and D.S. Dolling. *Tactical Missile Aerodynamics: General Topics*, volume I, chapter Swept Shock Wave/Boundary-Layer Interactions. AIAA, 1997.
- ⁸D.D. Knight and G. Degrez. Shock Wave Boundary Layer Interactions in High Mach Number Flows – A Critical Survey of Current CFD Prediction Capabilities. Technical report, AR-319, Vol. 2, AGARD, 1997.
- ⁹A. Zheltovodov. Some advances in research of shock wave turbulent boundary layer interactions. *AIAA Paper 2006-496*, 2006.
- ¹⁰D.S. Dolling. Fifty years of shock wave/boundary layer interaction research: what next? *AIAA J.*, 39(8), 2001.
- ¹¹H. Babinsky and J.K. Harvey, editors. *Shock Wave-Boundary Layer Interactions*. Cambridge University Press, 2011.
- ¹²P. Doerffer, C. Hirsch, J.-P. Dussauge, H. Babinsky, and G.N. Barakos, editors. *Unsteady Effects of Shock Wave Induced Separation*. Notes on Numerical Fluid Mechanics and Multidisciplinary Design. Springer, 2010.
- ¹³G.S. Settles and L.J. Dodson. Supersonic and Hypersonic Shock/Boundary-Layer Interaction Database. *AIAA Journal*, 32(7):1377–1383, July 1994.
- ¹⁴M.I. Kussoy and K.C. Horstman. Documentation of Two- and Three-Dimensional Shock-Wave/Turbulent-Boundary-Layer Interaction Flows at Mach 8.2. Technical Report 103838, NASA, Ames Research Center, Moffet Field, California 94035-1000, May 1991.
- ¹⁵D.S. Dolling. Problems in the Validation of CFD Codes Through Comparison with Experiment. In *AGARD Symposium on Theoretical and Experimental Methods in Hypersonic Flows*. Turin, Italy, 1992.
- ¹⁶J.-P. Dussauge, P. Dupont, and J.-F. Debieve. Unsteadiness in shock wave boundary layer interactions with separation. *Aerospace Science and Technology*, 10:85–91, 2006.
- ¹⁷J.K. Wideman, J.L. Brown, J.B. Miles, and O. Ozcan. Skin-Friction Measurements in a Three-Dimensional, Supersonic Shock-Wave/Boundary-Layer Interaction. *AIAA Journal*, 33(5):805–811, May 1995.
- ¹⁸C. P. Goyne, McDaniel J. C., T. M. Quagliaroli, R. H. Krauss, and S. W. Day. Dual-mode combustion of hydrogen in a mach 5 continuous-flow facility. *J. Prop. Power*, 17(6):1313, 2001.
- ¹⁹D. J. Dolvin. Hypersonic international flight research and experimentation (hifire) fundamental sciences and technology development strategy. In *15th AIAA International Space Planes and Hypersonic Systems and Technologies Conference*, April 2008. Dayton, Ohio; AIAA-2008-2581.
- ²⁰D. Adamczak, R. Kimmel, A. Paull, and H. Alesi. Hifire-1 flight trajectory estimation and initial experimental results. *AIAA Paper 2011-2358*, 2011.
- ²¹R. Kimmel and D. Adamczak. Hifire-1 background and lessons learned. *AIAA Paper 2012-1088*, 2012.
- ²²M. Gruber, K. Jackson, T. Jackson, and J. Liu. Hydrocarbon-fueled scramjet combustor flowpath development for mach 6–8 hifire flight experiment. *55th JANNAF Propulsion Meeting*, Boston, MA, 2008.
- ²³Kevin R. Jackson, Mark R. Gruber, and Salvatore Buccellato. Hifire flight 2 overview and status update 2011. In *17th AIAA International Space Planes and Hypersonic Systems and Technologies Conference*, April 2011. AIAA 2011-2202.
- ²⁴K. Cabell, N. Hass, A. Storch, and M. Gruber. Hifire direct-connect rig (hdcr) phase i scramjet test results from the nasa langley arc-heated scramjet test facility. In *17th AIAA International Space Planes and Hypersonic Systems and Technologies Conference*, April 2011. San Francisco, California; AIAA 2011-2248.
- ²⁵K. Jackson, M. Gruber, and S. Buccellato. Hifire flight 2 - a program overview. In *51st AIAA Aerospace Sciences Meeting*, number AIAA 2013-0695. AIAA, January 2013.
- ²⁶Z.R. Murphree, K.B. Yuceil, N.T. Clemens, and D.S. Dolling. Experimental studies of transitional boundary layer shock wave interactions. *AIAA Paper 2007-1139*, 2007.
- ²⁷S. Teramoto. Large-eddy simulation of transitional boundary layer with impinging shockwave. *AIAA J.*, 43(11):2354–2363, 2005.
- ²⁸D.S. Dolling and C.T. Or. Unsteadiness of the shock wave structure in attached and separated compression ramp flows. *Expts. in Fluids*, 3:24–32, 1985.
- ²⁹R.A. Gramann and D.S. Dolling. Detection of turbulent boundary-layer separation using fluctuating wall pressure signals. *AIAA J.*, 28:1052–1056, 1990.
- ³⁰J.C. Gonzalez and D.S. Dolling. Correlation of interaction sweepback effects on the dynamics of shock-induced turbulent separation. *AIAA Paper 93-0776*, 1993.
- ³¹K. C. Muck, J. P. Dussauge, and S. M. Bogdonoff. Structure of the wall pressure fluctuations in a shock-induced separated turbulent flow. *AIAA Paper 85-0179*, 1985.
- ³²L.J. Souverein, P. Dupont, J.-F. Debieve, J.-P. Dussauge, J.-P. van Oudheusden, and F. Scarano. Effect of interaction strength on unsteadiness in turbulent shock-wave-induced separations. *AIAA J.*, 48(7):1480–1493, July 2010.

- ³³T.C. Adamson and A.F. Messiter. Analysis of two-dimensional interactions between shock waves and boundary layers. *Ann. Rev. Fluid Mech.*, 12:103–138, 1980.
- ³⁴R. Yentsch and D. Gaitonde. Evaluation of a rans model for analysis of the hifire-1 flight test. *Journal of Spacecraft and Rockets*, 2013 (Accepted).
- ³⁵D.V. Gaitonde, P.W. Canupp, and M.S. Holden. Heat transfer predictions in a laminar hypersonic viscous/inviscid interaction. *Journal of Thermophysics and Heat Transfer*, 16(4), Oct-Dec 2002.
- ³⁶M.S. Holden and T.P. Wadhams. Code validation study of laminar shock/boundary layer and shock/shock interactions in hypersonic flow. part a: Experimental measurements. *AIAA Paper 2001-1031*, Jan 2001.
- ³⁷J.K Harvey, M.S. Holden, and T.P. Wadhams. Code validation study of laminar shock/boundary layer and shock/shock interactions in hypersonic flow. part b: Comparison with navier-stokes and dsmc solutions. *AIAA Paper 2001-1031*, Jan 2001.
- ³⁸B. Edney. Anomalous Heat Transfer and Pressure Distributions on Blunt Bodies at Hypersonic Speeds in the Presence of an Impinging Shock. Technical Report 115, The Aeronautical Research Institute of Sweden, Stockholm, February 1968.
- ³⁹J. Delery and J.G. Marvin. Shock-Wave Boundary Layer Interactions. *AGARD Report No. 280*, 1986.
- ⁴⁰N. Titchener and H. Babinsky. Shock wave/boundary-layer interaction control using a combination of vortex generators and bleed. *AIAA J.*, 51(5):1221–1233, 2013.
- ⁴¹E. Garnier. Stimulated detached eddy simulation of three-dimensional shock / boundary layer interaction. *Shock Waves*, 19:479–486, 2009.
- ⁴²D. Mee and R. Stalker. Investigation of Weak Shock-Shock and Shock-Expansion Intersection in the Presence of a Turbulent Boundary Layer. *AIAA Paper 87-0549*, 1987.
- ⁴³D. Gaitonde and D. Knight. Numerical Investigation of Some Control Methods for 3-D Turbulent Interactions Due to Sharp Fins. *AIAA Paper 89-0360*, 1989.
- ⁴⁴M.I. Kussoy, K.C. Horstman, and C.C. Horstman. Hypersonic Crossing Shock-Wave/Turbulent-Boundary-Layer Interactions. *AIAA Journal*, 31(12):2197–2203, 1993.
- ⁴⁵D. Gaitonde and J.S. Shang. The Structure of a Double-Fin Turbulent Interaction at Mach 4. *AIAA J.*, 33(12):2250–2258, Dec. 1995.
- ⁴⁶D. Gaitonde, J.S. Shang, and M.R. Visbal. Structure of a Double-Fin Turbulent Interaction at High Speed. *AIAA Journal*, 33(2):193–200, Feb. 1995.
- ⁴⁷D. Gaitonde, J.S. Shang, T.J. Garrison, A.A. Zheltovodov, and A.I. Maksimov. Three-Dimensional Turbulent Interactions Caused by Asymmetric Crossing-Shock Configurations. *AIAA J.*, 37(12):1602–1608, 1999.
- ⁴⁸T.J. Garrison and G.S. Settles. Laser Interferometer Skin-Friction Measurements of Crossing-Shock Wave/Turbulent Boundary-Layer Interactions. *AIAA Paper 93-3072*, 1993.
- ⁴⁹A.A. Zheltovodov and A.I. Maksimov. Hypersonic Crossing-Shock-Waves/Turbulent Boundary Layer Interactions. Technical Report Final Report, EOARD Contract F61775-98-WE091, Russian Academy of Sciences, Novosibirsk, Russia, 1999.
- ⁵⁰J.D. Schmisser and D.V. Gaitonde. Numerical investigation of strong crossing shock-wave/turbulent boundary-layer interactions. *AIAA Journal*, 39(9):1742–1749, Sep. 2001.
- ⁵¹J.D. Schmisser and D.V. Gaitonde. Numerical simulation of mach reflection in steady flows. *Shock Waves*, 21(6):499–509, 2011.
- ⁵²D. Knight, C. Horstman, B. Shapey, and S. Bogdonoff. Structure of Supersonic Turbulent Flow Past a Sharp Fin. *AIAA Journal*, 25:1331–1337, October 1987.
- ⁵³D. Gaitonde, J.S. Shang, and J.R. Edwards. Structure of a Supersonic Three-Dimensional Cylinder/Offset-Flare Turbulent Interaction. *Journal of Spacecraft and Rockets*, 34(3):294–302, 1997.
- ⁵⁴L. Trilling. Oscillating shock boundary-layer interaction. *J. Aerosp. Sc.*, 25(5):301–304, 1958.
- ⁵⁵N. Mullenix and D. Gaitonde. Analysis of unsteady behavior in shock/turbulent boundary layer interactions with large-eddy simulations. *AIAA Paper 2013-404*, 10.2514/6.2013-404, 2013.
- ⁵⁶N. Webb, C. Clifford, and M. Samimy. Preliminary results on shock wave/boundary layer interaction control using localized arc filament plasma actuators. *AIAA Paper 2011-3426*, 2011.
- ⁵⁷N. Webb, C. Clifford, and M. Samimy. An investigation of the control mechanism of plasma actuators in a shock wave-boundary layer interaction. *AIAA Paper 2013-402*, 2013.
- ⁵⁸B. Ganapathisubramani, N. Clemens, and D. Dolling. Effects of upstream boundary layer on the unsteadiness of shock-induced separation. *J. Fluid Mech.*, 585:369–394, 2007.
- ⁵⁹P. Dupont, S. Piponnai, A. Sidorenko, and J.F. Debieve. Investigation by particle image velocimetry measurements of oblique shock reflection with separation. *AIAA J.*, 46:1365–1370, 2008.
- ⁶⁰S. Piponnai, E. Collin, P. Dupont, and J.F. Debieve. Simultaneous wall pressure - piv measurements in a shock wave/turbulent boundary layer interaction. *Seventh International Symposium on Turbulence and Shear Flow Phenomena (TSFP-7)*, 2011.
- ⁶¹H. Kubota and J. Stollery. An Experimental Study of the Interaction Between a Glancing Shock Wave and a Turbulent Boundary Layer. *Journal of Fluid Mechanics*, 116:431–458, 1982.
- ⁶²R. Kimmel, D. Adamczak, A. Paull, R. Paull, J. Shannon, R. Pietsch, M. Frost, and H. Alesi. Hifire-1 preliminary aerothermodynamic measurements. *AIAA Paper 2011-3413*, 2011.
- ⁶³P. Bookey, C. Wyckham, A. Smits, and M.P. Martin. New experimental data of stbli at dns/les accessible reynolds numbers. *AIAA Paper 2005-309*, 2005.
- ⁶⁴N.A. Adams. Direct simulation of the turbulent boundary layer along a compression ramp at $m=3$ and $re_\theta = 1685$. *J. Fluid Mech.*, 420:47–83, 2000.
- ⁶⁵S. Pirozzoli and F. Grasso. Direct numerical simulation of impinging shock wave/turbulent boundary layer interactionat $m=2.25$. *Phys. Fluids*, 18, 2006.
- ⁶⁶M. Wu and M.P. Martin. Direct numerical simulation of supersonic turbulent boundary layer over a compression ramp. *AIAA J.*, 45:879–889, 2007.
- ⁶⁷S. Pirozzoli, A. Beer, M. Bernardini, and F. Grasso. Computational analysis of impinging shock-wave boundary layer interaction under conditions of incipient separation. *Shock Waves*, 19:487–497, 2009.

- ⁶⁸S. Priebe and M.P. Martin. Direct numerical simulation of a reflected-shock-wave/ turbulent-boundary-layer interaction. *AIAA J.*, 47(5):1173–1185, 2009.
- ⁶⁹E. Touber and N.D. Sandham. Large-eddy simulation of low-frequency unsteadiness in a turbulent shock-induced separation bubble. *Theor. Comput. Fluid Dyn.*, 23:79–107, 2009.
- ⁷⁰E. Touber and N.D. Sandham. Comparison of three large-eddy simulations of shock-induced turbulent separation bubbles. *Shock Waves*, 19:469–478, 2009.
- ⁷¹B. Morgan, S. Kawai, and S.K. Lele. A parametric investigation of oblique shockwave/turbulent boundary layer interaction using les. *AIAA 2011-3430*, 2011.
- ⁷²S. Priebe and M.P. Martin. Low-frequency unsteadiness in shock wave-turbulent boundary layer interaction. *J. Fluid Mech.*, 699:1–49, 2012.
- ⁷³S. Priebe and M.P. Martin. Low-frequency unsteadiness in dns of shock wave/turbulent boundary layer interaction. *AIAA Paper 2011-725*, 2011.
- ⁷⁴L. Agostini, L. Larcheveque, P. Dupont, J.-F. Denieve, and J-P. Dussauge. Zones of influence and shock motion in a shock/boundary layer interaction. *AIAA J.*, 50(6), 2012.
- ⁷⁵K. C. Kim and R. J. Adrian. Very large-scale motion in the outer layer. *Phys. Fluids*, 11:417–422, 1999.
- ⁷⁶P. Dupont, C. Haddad, and J. F. Debieve. Space and time organization in a shock induced boundary layer. *J. Fluid Mech.*, 2006.
- ⁷⁷S. Piponnau, J.P. Dussauge, J.F. Debieve, and P. Dupont. A simple model for low-frequency unsteadiness in shock-induced separation. *Journal of Fluid Mechanics*, 629:87–108, 2009.
- ⁷⁸E. Touber and N.D. Sandham. Low-order stochastic modelling of low-frequency motions in reflected shock-wave/boundary-layer interactions. *J. Fluid Mech.*, 671:417–465, 2011.
- ⁷⁹B. Ganapathisubramani, N.T. Clemens, and D.S. Dolling. Low-frequency dynamics of shock-induced separation in a compression ramp interaction. *J. Fluid Mech.*, 636:397–425, 2009.
- ⁸⁰K.J. Plotkin. Shock wave oscillation driven by turbulent boundary layer fluctuations. *AIAA J.*, 13(8):1036–1040, 1975.
- ⁸¹J. Poggie and A.J. Smits. Shock unsteadiness in a reattaching shear layer. *J. Fluid Mech.*, 429:155–185, 2001.
- ⁸²J. Poggie and A.J. Smits. Experimental evidence for plotkin model of shock unsteadiness in separated flow. *Phys. Fluids*, 17:018107, 2005.
- ⁸³J. Poggie, N. Bisek, R.L. Kimmel, and S.A. Stanfield. Spectral characteristics of separation shock unsteadiness. *AIAA Paper (to be presented)*, *Fluid Dynamics Conference, San Diego*, 2013.
- ⁸⁴U. Dallmann. Three-Dimensional Vortex Structures and Vorticity Topology. *Fluid Dynamics Research, The Japan Society of Fluid Mechanics*, 3:183–189, 1988.
- ⁸⁵M. Tobak and D.J. Peake. Topology of Three-Dimensional Separated Flows. *Annual Review of Fluid Mechanics*, 14:61–85, 1982.
- ⁸⁶A. Perry and M. Chong. A Description of Eddying Motions and Flow Patterns Using Critical-Point Concepts. *Ann. Rev. Fluid Mech.*, 19:125–155, 1987.
- ⁸⁷A.A. Zheltovodov, Maksimov A.I., Shevchenko A.M., and Knight D.D. 3-D Separation topology in asymmetric crossing shock waves and expansion fans/turbulent boundary layer interaction conditions. *Thermophysics and Aeromechanics*, V.4, 1998.
- ⁸⁸B. Morgan, J. Larsson, S. Kawai, and S.K. Lele. Improving low-frequency characteristics of recycling/rescaling inflow turbulence generation. *AIAA J.*, 49(3):582–597, 2011.
- ⁸⁹M.M. Rai, T.B. Gatski, and G. Erlebacher. Direct simulation of spatially evolving compressible turbulent boundary layers. *AIAA Paper 85-0583*, 1995.
- ⁹⁰D.P. Rizzetta, M.R. Visbal, and D.V. Gaitonde. Large-eddy simulation of supersonic compression-ramp flow by high-order method. *AIAA J.*, 39(12):2283–2292, 2001.
- ⁹¹N. Mullenix, D.V. Gaitonde, and M.R. Visbal. Generation of a spatially developing supersonic turbulent boundary layer with a body force-based method. *AIAA Journal*, 2013 (Accepted).
- ⁹²M.R. Visbal. Strategies for control of transitional and turbulent flows using plasma-based actuators. *International Journal of CFD*, 24(7), 2010.
- ⁹³K. Tani and D.S. Dolling. Fluctuating Wall Pressures in a Mach 5 Crossing Shock/Turbulent Boundary Layer Interaction Including Asymmetric Effects. *AIAA Paper 96-0045*, Jan. 1996.
- ⁹⁴R.A. Gramann and D.S. Dolling. Unsteady Separation in Shock Wave Turbulent Boundary Layer Interactions. *AIAA Paper 86-1033*, 1986.
- ⁹⁵J. D. Schmisseur and D. S. Dolling. Fluctuating wall pressures near separation in highly swept turbulent interactions. *AIAA J.*, 32:1151–1157, 1994.
- ⁹⁶Y. Hou, O.H. Unalmis, P.C. Bueno, N. T. Clemens, and D. S. Dolling. Effects of boundary-layer velocity fluctuations on unsteadiness of blunt-fin interactions. *AIAA J.*, 42:2615–2619, 2004.
- ⁹⁷D.M. Bushnell and L.M. Weinstein. Correlation of peak heating for reattachment of separated flows. *J. Spacecraft and Rockets*, 5(9):1111–1112, 1968.
- ⁹⁸M.S. Holden. Shock wave-turbulent boundary layer interaction in high speed flow. Technical Report ARL TR 75-0204, CALSPAN Corporation, Buffalo, NY, June 1975.
- ⁹⁹M.S. Holden and J.R. Moselle. A database of aerothermal measurements in hypersonic flow for cfd validation. *AIAA Paper 92-4023*, 1992.
- ¹⁰⁰M.S. Holden, J.R. Moselle, S.J. Sweet, and S.C. Martin. A database of aerothermal measurement in hypersonic flow for cfd validation. *AIAA Paper 96-4597*, 1996.
- ¹⁰¹E. R. Van Driest. Turbulent boundary layer in compressible fluids. *J. Aero. Sc.*, 18(3):145–160, 1951.
- ¹⁰²E.R.G. Eckert. Engineering relations for friction and heat transfer to surfaces in high velocity flow. *J. of the Aero. Sc.*, 22:585–587, 1955.
- ¹⁰³T.J. Garrison, G.S. Settles, and C.C. Horstman. Measurements of the Triple Shock/Wave Turbulent Boundary-Layer Interaction. *AIAA Journal*, 34(1):57–64, Jan. 1996.
- ¹⁰⁴M.S. Holden and T.P. Wadhams. A database of aerothermal measurements in hypersonic flow in "building block experiments for cfd validation. *AIAA Paper 2003-1137*, 2003.
- ¹⁰⁵G.V. Candler, I. Nompelis, and M.-C. Druguet. Navier-stokes predictions of hypersonic double-cone and cylinder-flare flow fields. *AIAA Paper 2001-1024*, Jan. 2001.

- ¹⁰⁶P.A. Gnoffo. Cfd validation studies for hypersonic flow prediction. *AIAA Paper 2001-1025*, Jan 2001.
- ¹⁰⁷H. Kato and J.C. Tannehill. Computation of hypersonic laminar separated flows using an iterated pns algorithm. *AIAA Paper 2001-1028*, Jan 2001.
- ¹⁰⁸J.N. Moss. Dsmc computations for regions of shock/shock and shock/boundary layer interaction. *AIAA Paper 2001-1027*, Jan. 2001.
- ¹⁰⁹I.D. Boyd and W.-L. Wang. Monte carlo computations of hypersonic interacting flows. *AIAA Paper 2001-1029*, Jan 2001.
- ¹¹⁰D. D'Ambrosio. Numerical prediction of laminar shock/shock interactions in hypersonic flow. *AIAA Paper 2002-1*, 2002.
- ¹¹¹I. Nompelis, G. V. Candler, and Holden M. S. Effect of vibrational nonequilibrium on hypersonic double-cone experiments. *AIAA Journal*, 41(11):2162–2169, 2003.
- ¹¹²I. Nompelis, G.V. Candler, M. MacLean, T.P. Wadhams, and M.S. Holden. Numerical investigation of high enthalpy chemistry on hypersonic double-cone experiments. *AIAA Paper 2005-584*, 2005.
- ¹¹³M. MacLean, M. Holden, T. Wadhams, and R. Parker. A computational analysis of thermochemical studies in the lens facilities. *AIAA Paper 2007-0121*, 2007.
- ¹¹⁴M.J. Wright, J. Sinha, K. Olejniczak, G.V. Candler, T.D. Magruder, and A.J. Smits. Numerical and experimental investigation of double-cone shock interactions. *AIAA Journal*, 38(12):2268–2276, Dec. 2000.
- ¹¹⁵M. Holden, T. Wadhams, and M. MacLean. Experimental studies in the lens supersonic and hypersonic tunnels for hypervelocity vehicle performance and code validation. *AIAA Paper 2008-2505*, 2008.
- ¹¹⁶D.D. Knight, J. Longo, D. Drikakis, D.V. Gaitonde, A. Lani, I. Nompelis, B. Reimann, and L. Walpot. Assessment of cfd capability for prediction of hypersonic shock interactions. *Progress in Aerospace Sciences*, 48-49:8–26, 2012.
- ¹¹⁷D.V. Gaitonde. An assessment of cfd for prediction of 2-d and 3-d high-speed flows. *AIAA Paper 2010-1284*, 2010.
- ¹¹⁸S. Karl, J. Martinez Schramm, and K. Hannemann. High enthalpy cylinder flow in heg: A basis for cfd validation. *AIAA Paper 2003-4252*, 2003.
- ¹¹⁹T.J. Coakley and P.G. Huang. Turbulence Modeling For High Speed Flows. *AIAA Paper 92-0436*, Jan. 1992.
- ¹²⁰A. Sinha, K. Mahesh, and G.V. Candler. Modeling shock unsteadiness in shock/turbulence interaction. *Phys. Fluids*, 15:2290–2297, 2003.
- ¹²¹D.C. Wilcox. *Turbulence Modeling for CFD*. DCW Industries, Inc, 2006.
- ¹²²C.J. Roy and F. G. Blottner. Review and assessment of turbulence models for hypersonic flows: 2d/axisymmetric cases. *AIAA Paper 2006-713*, 2006.
- ¹²³J.R. DeBonis, W.L. Oberkampf, R. T. Wolf, P.D. Orkwis, M. G. Turner, H. Babinsky, and J.A. Benek. Assessment of computational fluid dynamics and experimental data for shock boundary-layer interactions. *AIAA Journal*, 50:891–903, 2012. 10.2514/1.J051341.
- ¹²⁴D. Bose, J.L. Brown, D.K. Prabhu, P. Gnoffo, C.O. Johnston, and B. Hollis. Uncertainty assessment of hypersonic aerothermodynamics prediction capability. *J. Spacecraft and Rockets*, 50(1), 2013. DOI:10.2514/1.A32268.
- ¹²⁵P. A. Gnoffo, S. A. Berry, and J. W. Van Norman. Uncertainty assessments of hypersonic shock wave-turbulent boundary-layer interactions at compression corners. *J. Spacecraft and Rockets*, 50(1), 2013. DOI:10.2514/1.A32250.
- ¹²⁶J.L. Brown. Hypersonic shock wave impingement on turbulent boundary layers: Computational analysis and uncertainty. *J. Spacecraft and Rockets*, 50(1):96–123, 2013. DOI:10.2514/1.A32250.
- ¹²⁷T. P. Wadhams, E. Mundy, M. G. MacLean, and M. S. Holden. Ground test studies of the hifire-1 transition experiment part 1: Experimental results. *J. Spacecraft and Rockets*, 45:1134–1148, 2008.
- ¹²⁸K.T. Berger, F. A. Greene, R. Kimmel, C. Alba, and H. Johnson. Aerothermodynamic testing and boundary-layer trip sizing of the hifire flight 1 vehicle. *J. Spacecraft and Rockets*, 45:1117–1124, 2008.
- ¹²⁹M. MacLean, T. Wadhams, M. Holden, and H. Johnson. Ground test studies of the hifire-1 transition experiment part 2: Computational analysis. *Journal of Spacecraft and Rockets*, 45:1149–1164, 2008.
- ¹³⁰R.J. Yentsch and D.V. Gaitonde. Numerical investigation of hypersonic phenomena encountered in hifire flight 1. *AIAA Paper 2012-0943*, 2012.
- ¹³¹X. Xiao, J.R. Edwards, and H.A. Hassan. Blending functions in hybrid large-eddy / reynolds-averaged navier-stokes simulations. *AIAA J.*, 42(12):2508–2515, 2004.
- ¹³²T.C. Fan, J.R. Edwards, H.A. Hassan, and R.A. Baurle. Hybrid large-eddy / reynolds-averaged navier-stokes simulations of shock-separated flows. *J. Spacecraft and Rockets*, 41(6):897–906, 2004.
- ¹³³S. Ghosh, J.-I. Choi, and J.R. Edwards. Simulation of shock boundary layer interactions with bleed using immersed boundary methods. *J. Prop. Power*, 26(2):203–214, 2010.
- ¹³⁴S. Ghosh, J.-I. Choi, and J.R. Edwards. Numerical simulation of the effects of mesoflaps in controlling shock / boundary layer interactions. *J. Prop. Power*, 28(5):955–970, 2012.
- ¹³⁵X. Xiao, J.R. Edwards, H.A. Hassan, and R.A Baurle. Inflow boundary conditions for hybrid large-eddy / reynolds-averaged navier-stokes simulations. *AIAA J.*, 41(8):1481–1490, 2003.
- ¹³⁶J.R. Edwards, J.-I. Choi, and J.A. Boles. Hybrid large-eddy / reynolds-averaged navier-stokes simulation of a mach-5 compression corner interaction. *AIAA J.*, 46(4):977–991, 2008.
- ¹³⁷D. Gieseking and J.R. Edwards. Simulations of a mach 3 compression-ramp interaction using les/rans models. *AIAA J.*, 50(10):2057–2068, 2012.
- ¹³⁸J.A. Boles and J.R. Edwards. Hybrid large-eddy / reynolds-averaged navier-stokes simulation of a mach 8.3 crossing-shock interaction. *AIAA Paper 2006-3039*, 2006.
- ¹³⁹F. Thivet, D.D. Knight, A.A. Zheltovodov, and A.I. Maksimov. Some insights in turbulence modeling for crossing-shock-wave/boundary-layer interactions. *AIAA Paper 2000-0131*, Jan. 2000.
- ¹⁴⁰S. Srikant, J. L. Wagner, A. Valdivia, M. R. Akella, and N. Clemens. Unstart detection in a simplified-geometry hypersonic inlet-isolator flow. *J. Prop. Power*, 26:1059–1071, 2010.
- ¹⁴¹J. L. Wagner, K. B. Yuceil, A. V Valdivia, N. T. Clemens, and D. S. Dolling. Experimental investigation of unstart in an inlet/isolator model in mach 5 flow. *AIAA J.*, 47:1528–1542, 2009.
- ¹⁴²R. Yentsch and D. Gaitonde. Numerical investigation of the hifire-2 scramjet flowpath. *AIAA Paper 2013-119*, 2013.

- ¹⁴³J. Boles, J. Edwards, J-I. Choi, and R. Baurle. Simulations of high-speed internal flows using les/rans models. *AIAA Paper 2009-1324*, 2009.
- ¹⁴⁴J. Boles, M. Hagenmaier, and K-Y. Hsu. Analysis of hybrid les / rans simulations of a back-pressured supersonic isolator. *AIAA Paper 2011-5825*, 2011.
- ¹⁴⁵P. Cocks, J. Donohue, C. Bruno, and M. Haas. Iddes of a dual-mode ethylene fueled cavity flameholder with an isolator shock train. *AIAA Paper 2013-116*, 2013.
- ¹⁴⁶M. Brown, D. Barone, T. Barhorst, D. Eklund, M. Gruber, T. Mathur, and R. Milligan. Tdlas-based measurements of temperature, pressure, and velocity in the isolator of an axisymmetric scramjet. *AIAA Paper 2010-6989*, 2010.
- ¹⁴⁷J. L. Wagner, K. B. Yuceil, and N. T. Clemens. Velocimetry measurements of unstart of an inlet-isolator model in mach 5 flow. *AIAA J.*, 48:1875–1888, 2010.
- ¹⁴⁸K.E. Hutchins, M.R. Akella, N.T. Clemens, and J.M. Donbar. Detection and transient dynamics modeling of experimental hypersonic inlet unstart. *AIAA Paper 2012-2808*, 2012.
- ¹⁴⁹N. Hass, K. Cabell, and A. Storch. Hifire direct-connect rig (hdcr) phase i ground test results from the nasa langley arc-heated scramjet test facility. In *JANNAF 43rd Combustion; 31st Airbreathing Joint Meeting*, pages 1–24. NASA Langley, ATK Space Systems, 2010.
- ¹⁵⁰P.G. Ferlemann. Forebody and inlet design for the hifire 2 flight test. *55th JANNAF Propulsion Meeting, Boston, MA*, 2008.
- ¹⁵¹Andrea M. Storch, Michael Bynum, Jiwen Liu, and Mark Gruber. Combustor operability and performance verification for hifire flight 2. In *17th AIAA International Space Planes and Hypersonic Systems and Technologies Conference*, April 2011. San Francisco, California; AIAA-2011-2249.
- ¹⁵²M. Bynum and R. A. Baurle. Design of experiments study for the hifire flight 2 ground test computational fluid dynamics results. *AIAA Paper 2011-2203*, 2011.
- ¹⁵³J. Liu and M. Gruber. Preliminary preflight cfd study on the hifire flight 2 experiment. *AIAA Paper 2011-2204*, 2011.
- ¹⁵⁴M.S. Holden, T.P. Wadhams, M. MacLean, A. Dufrene, E. Mundy, and E. Marineau. A review of basic research and development programs conducted in the lens facilities in hypervelocity flows. *AIAA Paper 2012-0469*, 2012.
- ¹⁵⁵T. Kouchi, C.P. Goyne, R.D. Rockwell Jr., R. Reynolds, R. Krauss, and J.C. McDaniel. Focusing-schlieren visualization in direct-connect dual-mode scramjet. *AIAA Paper 2012-5834*, 2012.
- ¹⁵⁶J.M. Donbar, M.S. Brown, G.J. Linn, and K-Y. Hsu. Simultaneous high-frequency pressure and tdlas measurements in a small-scale axisymmetric isolator with bleed. *2012-0331*, 2012.
- ¹⁵⁷D.V. Gaitonde and D.D. Knight. A numerical investigation of effect of bleed on 3-d turbulent interactions due to sharp fins. *AIAA Journal*, 29(11), Nov. 1991.
- ¹⁵⁸B. Croker. Numerical investigation of 3-d swept shock interaction control with porous surfaces. *AIAA Paper 2006-3346*, 2006.
- ¹⁵⁹E. S. Hafnerichter, Y. Lee, J. C. Dutton, and E. Loth. Normal shock/boundary layer interaction control using aeroelastic mesoflaps. *AIAA J.*, 19(3):464–472, 2003.
- ¹⁶⁰H.A. Holden and H. Babinsky. Separated shock-boundary-layer interaction control using streamwise slots. *J. Aircraft*, 42(1):166–171, 2005.
- ¹⁶¹H. Ogawa and H. Babinsky. Shock/boundary layer interaction control using three-dimensional bumps in supersonic engine inlet. *AIAA Paper 2008-599*, 2008.
- ¹⁶²P.L. Blinde, B.W. van Oudheusden, and F. Scarano. Effects of micro-ramps on a shock wave/turbulent boundary layer interaction. *Shock Waves*, 19:507–520, 2009.
- ¹⁶³S. Lee and E. Loth. Impact of ramped vanes on normal shock boundary layer interaction. *AIAA J.*, 50:2069–2079, 2012.
- ¹⁶⁴J.M. Oorebeek, W.R. Nolan, and H. Babinsky. Comparison of bleed and micro-vortex generator effects on supersonic boundary-layers. *AIAA Paper 2012-0045*, 2012.
- ¹⁶⁵R. Kumar, M.Y. Ali, F.S. Alvi, and L. Venkatakrishnan. Generation and control of oblique shocks using microjets. *AIAA J.*, 49(12):2751–2759, 2011.
- ¹⁶⁶M.Y. Ali, F.S. Alvi, C. Manisankar, S.B. Verma, and L. Venkatakrishnan. Studies on the control of shock wave-boundary layer interaction using steady microactuators. *AIAA Paper 2011-3425*, 2011.
- ¹⁶⁷S.B. Verma and C. Manisankar. Shockwave/boundary-layer interaction control on a compression ramp using steady microjets. *AIAA J.*, 50(12):2573–2764, 2012.
- ¹⁶⁸E. Caraballo, N. Webb, J. Little, J.-H. Kim, and M. Samimy. Supersonic inlet control using plasma actuators. *AIAA Paper 2009-0924*, 2009.
- ¹⁶⁹V. Jaunet, J. F. Debieve, and P. Dupont. Experimental investigation of an oblique shock reflection with separation over a heated wall. *AIAA Paper 2012-1095*, 2012.
- ¹⁷⁰M. Nishihara, D. Gaitonde, and I.V. Adamovich. Effect of nanosecond pulse discharges on oblique shock and shock wave-boundary layer interaction. *AIAA Paper 2013-0461*, 2013.
- ¹⁷¹N.J. Bisek, D.P. Rizzetta, and J. Poggie. Plasma control of a turbulent shock boundary-layer interaction. *AIAA J., Early Edition*, 2013.
- ¹⁷²D. V. Gaitonde and J. H. Miller. Eddy-current-based momentum transfer method to suppress three-dimensional separation. *AIAA Journal*, 43(5):1064–1074, May 2005.
- ¹⁷³S. Leonov, V. Bityurin, K. Savelkin, and D. Yarantsev. Effect of electrical discharge on separation processes and shocks position in supersonic airflow. *AIAA Paper 2002-3055*, 2002.
- ¹⁷⁴S.V. Bobashev, A.V. Erofeev, T.A. Lapushkina, S.A. Poniatov, R.V. Vasili'eva, and D.M. van Wie. Effect of magnetohydrodynamics interaction in various parts of diffuser on inlet shocks: Experiment. *J. Prop. Power*, 21(5):831–837, 2005.
- ¹⁷⁵V. Narayanswamy, L.L. Raja, and N.T. Clemens. Control of a shock/boundary-layer interaction by using a pulsed-plasma jet actuator. *AIAA J.*, 50(1), 2012.
- ¹⁷⁶B.R. Greene, N.T. Clemens, and D. Micka. Control of shock boundary layer interaction using pulsed plasma jets. *AIAA Paper 2013-0405*, 2013.